



**POLITECNICO**  
MILANO 1863

SCUOLA DI INGEGNERIA INDUSTRIALE  
E DELL'INFORMAZIONE

# Adhesive Bonded Joints in Space: Technical Overview of Behavior, Modeling, and Application Prob- lems

TESI DI LAUREA MAGISTRALE IN  
AERONAUTICAL ENGINEERING - INGEGNERIA AERONAUTICA

Author: **Enrico Fiodo**

Student ID: 870211

Advisor: Prof. Antonio Mattia Grande

Co-advisors: Fabrizio Duò

Academic Year: 2024-25



# Abstract

Adhesively bonded joints have gained importance in the space industry due to their exceptional ability to transfer loads and bond dissimilar substrates. However, their successful integration into space structures requires extensive characterization of performance under various bonding conditions, including differences in surface preparation, material properties, and curing methods. This thesis presents a comprehensive investigation into the testing, simulation, and operational behavior of structural adhesives in space applications. The study employs a combination of experimental tests and advanced finite element simulations to investigate the complexities involved in accurately characterizing these joints. It also reveals the complexities and expenses associated with evaluating each bonding condition separately, which often limits the applicability of the results to specific substrates. The findings offer valuable insights into optimizing adhesive performance under the thermal and mechanical stresses encountered in space, ultimately guiding the design and reliable integration of adhesive joints in future aerospace structures.

**Keywords:** adhesive bonding; structural adhesives; adhesive testing; finite element analysis.



## Abstract in lingua italiana

I giunti adesivi hanno acquisito importanza nell'industria spaziale grazie alla loro eccezionale capacità di trasferire carichi e di incollare substrati dissimili. Tuttavia, il successo della loro integrazione nelle strutture spaziali richiede un'ampia caratterizzazione delle prestazioni in varie condizioni di incollaggio, comprese le differenze nella preparazione delle superfici, nelle proprietà dei materiali e nei metodi di indurimento. Questa tesi presenta un'indagine completa sui test, la simulazione e il comportamento operativo degli adesivi strutturali nelle applicazioni spaziali. Lo studio impiega una combinazione di test sperimentali e simulazioni avanzate agli elementi finiti per indagare le complessità legate alla caratterizzazione accurata di queste giunzioni. Inoltre, rivela le complessità e le spese associate alla valutazione di ogni condizione di incollaggio separatamente, che spesso limita l'applicabilità dei risultati a substrati specifici. I risultati offrono spunti per ottimizzare le prestazioni dell'adesivo in presenza di sollecitazioni termiche e meccaniche incontrate nello spazio, guidando in ultima analisi la progettazione e l'integrazione affidabile dei giunti adesivi nelle future strutture aerospaziali.

**Parole chiave:** incollaggio; adesivi strutturali; test a trazione; analisi agli elementi finiti.



# Contents

|   |            |
|---|------------|
| <b>Abstract</b>   | <b>i</b>   |
| <b>Abstract in lingua italiana</b>  | <b>iii</b> |
| <b>Contents</b>   | <b>v</b>   |
| <br>  |            |
| <b>Introduction</b>   | <b>1</b>   |
| 0.1 Golas . . . . .   | 2          |
| <b>1 Adhesive bonded joints</b>   | <b>3</b>   |
| 1.1 Failure criteria . . . . .  | 4          |
| 1.1.1 Stress distribution . . . . .   | 5          |
| 1.2 Substrate . . . . .   | 7          |
| 1.3 Type of adhesives . . . . .   | 7          |
| 1.3.1 Optical cements . . . . .   | 7          |
| 1.3.2 Structural adhesives . . . . .  | 8          |
| 1.4 Adhesive selection . . . . .  | 8          |
| 1.5 Market research . . . . .   | 10         |
| 1.6 Finite Element Analysis . . . . .   | 11         |
| 1.6.1 Finite element analysis of adhesive bonded joints using Simcenter<br>3D . . . . . | 11         |
| 1.6.2 Cohesive elements and their limitations . . . . .                                 | 14         |
| <b>2 Projects and simulations</b>   | <b>17</b>  |
| 2.1 Effects of the space environment on substrates and adhesives . . . . .              | 18         |
| 2.1.1 Effect of the space environment on Titanium and Invar structures .                | 18         |
| 2.1.2 Effect of the space environment on structural adhesives . . . . .                 | 18         |
| 2.2 Thermoelastic analysis . . . . .  | 19         |
| 2.3 Deformation of telescope lens . . . . .   | 20         |

|          |   |           |
|----------|---|-----------|
| <b>3</b> | <b>Structural adhesives</b>                               | <b>23</b> |
| 3.1      | EC2216 . . . . .  | 23        |
| 3.1.1    | Tensile test . . . . .                                    | 24        |
| 3.1.2    | Shear test . . . . .                                      | 28        |
| 3.1.3    | Static test on a lens in its barrel . . . . .             | 34        |
| 3.2      | EP42HT-2LTE . . . . .                                     | 36        |
| 3.2.1    | Tensile test . . . . .                                    | 36        |
| 3.2.2    | Shear test . . . . .                                      | 37        |
| 3.3      | Manufacturing and integration phase . . . . .             | 39        |
| 3.3.1    | Stress induced by the shrinkage of the adhesive . . . . . | 39        |
| 3.3.2    | Stress induced by the difference in CTE . . . . .         | 40        |
| 3.3.3    | Integration of the optical fibers . . . . .               | 43        |
| 3.4      | Considerations on Two-Component Epoxy Adhesives . . . . . | 45        |
| <b>4</b> | <b>Non structural adhesives</b>                           | <b>47</b> |
| 4.1      | Nusil CV1142 . . . . .                                    | 47        |
| 4.2      | Thermoelastic analysis: C2302 EAGLET . . . . .            | 49        |
| 4.3      | RTV566 . . . . .  | 54        |
| 4.4      | NOA 88 . . . . .  | 56        |
| 4.4.1    | Thermoelastic analysis . . . . .                          | 59        |
| <b>5</b> | <b>Conclusions and future developments</b>                | <b>61</b> |
|          | <b>Bibliography</b>                                       | <b>63</b> |
| <b>A</b> | <b>Appendix A</b>   | <b>67</b> |
| A.1      | Market research tables . . . . .                          | 67        |
| A.2      | Adhesive Datasheets . . . . .                             | 70        |
|          | <b>List of Figures</b>                                    | <b>71</b> |
|          | <b>List of Tables</b>                                     | <b>73</b> |
|          | <b>Acknowledgements</b>                                   | <b>75</b> |

# Introduction

Adhesively bonded joints are a growing priority in the space industry. They can reduce weight and improve structural performance by eliminating stress concentrations associated with mechanical bonds. Adhesive bonding enables robust connections between dissimilar materials, which is a critical advantage in modern spacecraft and satellite design. With stringent requirements for durability under extreme thermal cycling, radiation, and vacuum conditions, agencies such as NASA and ESA have increasingly focused on adhesive technologies to enhance the reliability and efficiency of space structures. This trend is driving continuous research and development aimed at optimizing adhesive performance for the demanding environments encountered in space.

The objective of this thesis is to analyze the characteristics and behavior of adhesives commonly employed in space applications. This research focuses on both structural and non-structural adhesives, with particular attention to the methods used to study, predict, and ultimately optimize adhesive performance under the extreme conditions encountered in space.

The initial section of this study presents a thorough review of adhesives, encompassing an examination of failure criteria and stress distribution mechanisms across diverse substrates. It also includes a discussion of factors that can enhance adhesive performance, with particular emphasis on the critical factors that must be considered when selecting an adhesive for specific aerospace projects. The study also incorporates market research to review the existing adhesive database in the context of space applications and to compare adhesives in use with new ones. Finally, this section introduces the analytical and simulation tools used to predict and assess the behavior of adhesively bonded joints.

The second part of the thesis shifts focus to practical evaluations. It presents a series of test simulations and case studies that address the challenges associated with using adhesives in space. These include issues related to structural integrity, manufacturing precision, and thermal elasticity. Both structural and non-structural adhesives are examined, and the necessity of thorough testing and simulation before deployment in flight projects is highlighted.

This thesis is based on direct experimental experience and advanced simulation techniques, offering insights that aim to bridge the gap between theoretical predictions and real-world performance in the demanding space environment.

## 0.1. Golas

This thesis work was done based on an internship: the company where I interned was OPTEC S.p.A., a company specializing in the production of telescopes for civil, military, ground, and space applications. During my experience, my work focused mainly on analyzing the behavior of the adhesives used to connect the telescope lens to its structure. Specifically, I studied the performance of these adhesives under the loads to which the telescope is subjected and the tough environmental conditions of space. A particular concern is the deformation of the delicate lenses supported by adhesives during both the operational life and the manufacturing process.

I have had the opportunity to actively participate in many phases of various projects, starting with the preliminary design and the choice of materials and ending with the final design, assembly, and structural analysis, especially following modifications to the original design.

# 1 | Adhesive bonded joints

Bonded joints use adhesives to join materials, offering advantages over traditional methods like welding or bolting. In optics, bonded joints are of interest to optomechanical engineers for creating stable assemblies. They differ from other types of joining primarily because the additive that creates the bond is a polymer rather than a metal. Heating the substrate (such as in soldering, brazing, and fusion welding) can reduce strength, cause deformation, and damage the material. The low or moderate temperatures involved in bonding have other advantages, such as not damaging the delicate optical substrate during manufacturing [22].

Compared with mechanical "spot" joints, such as rivets, clamps, and screws, which may have relatively high local stresses, an adhesive joint can carry loads over larger areas. Therefore, the strength, stiffness, energy absorption, and durability of a properly sized adhesive joint will be better. The uniform load distribution can also allow the material size to be reduced.

However, adhesive-bonded joints present several challenges:

- Sensitivity to peeling
- Need for surface treatment to ensure cleanliness, wetting, adhesion and corrosion resistance
- Need for fixation during curing and require limited handling
- Extreme temperatures limit some properties
- Difficult to ensure quality, strict process control required
- Dosage and accuracy during application can be challenging
- Health, environment, and safety (especially for curing adhesives)
- Disassembly and repair can be difficult
- Need for training in production

**Certification of adhesive joints:** Adhesive joints, despite their increasing use in structures, face certification challenges due to uncertainties in joint quality and limitations in nondestructive testing. Crack propagation in adhesive joints is also difficult to control at the design stage, making the use of reliable simulation models essential for certification, particularly for large-scale structures. Currently, certification methods focus on calculating the required bonding surface area or developing reliable testing methods [12].

## 1.1. Failure criteria

Adhesively bonded joints may fail by different mechanisms, which are broadly classified as adhesive, cohesive, or mixed-mode failures. Adhesive failure occurs when the bond between the adhesive and the substrate breaks down, often due to inadequate surface preparation or incompatible surface energies, resulting in separation with minimal adhesive residue remaining on the adherend. In contrast, cohesive failure occurs within the adhesive layer itself: when the intrinsic strength of a brittle adhesive is exceeded, the material fractures, leaving significant residue on both surfaces. Mixed-mode failure, on the other hand, is characterized by a combination of both mechanisms and typically arises under complex loading conditions that subject the joint simultaneously to tensile, shear, and peeling stresses. This leads to fracture surfaces that exhibit both debonding at the interface and internal rupture of the adhesive. The differentiation of these failure modes is possible through post-rupture examinations, with the presence or absence of adhesive remnants on the substrates serving as a key indicator.



Figure 1.1: Adhesive failure    Figure 1.2: Cohesive failure    Figure 1.3: Mixed failure

There are several failure criteria that are used to evaluate the integrity of the bonded joints, and various techniques are used to predict the maximum stress they can sustain. These methods can be broadly divided into analytical and numerical approaches ([22], [24]).

**Maximum Stress or Strain Criteria:** These are among the most popular and intuitive failure criteria for bonded joints. Failure is predicted when the maximum stress or strain at a critical point reaches a critical value. Like in the Volkersen model, where the adhesive

is assumed to deform only in shear, the maximum shear stress is used as a failure criterion [11].

**Maximum Shear Stress:** This criterion is often used in lap joints if the adhesive deforms primarily in shear [19].

**Maximum peel stress:** Peel stress should generally be minimized by design rather than used as a design limit. However, some approaches use maximum peel stress as a failure criterion, especially when distinguishing between failure in the adhesive and failure in the adherend [22]. In the case studied, this type of criterion is never used because the adhesive used and the geometries are less subject to peeling.

**Maximum Principal Tensile Stress and Strain:** These criteria are used to predict the failure of single-lap joints. The maximum principal tensile stress is the most responsible for the failure of joints bonded to brittle adhesives. This criterion is useful in our cases because we deal with brittle adhesives that allow little deformation and delamination before failure [27].

**Maximum Von Mises Stress:** The von Mises Yield Criterion simplifies complex multiaxial stress states into a single value that can be directly compared to the yield strength of a material, making it a practical method for predicting when and where an adhesive-bonded joint may begin to fail. By reducing the complex multiaxial stress state to a single scalar quantity ( $\sigma_{vm}$ ), it's possible to compare this calculated value directly to the yield strength of the adhesive obtained from uniaxial tests. For example, in some FEA studies of adhesive bonds, failure is predicted when the von Mises stress in the adhesive layer reaches a predetermined critical value, indicating the onset of cohesive failure. This criterion is widely used in our cases because of its conservative nature; by defining an allowable value through tensile tests on specimens, it is possible to determine a conservative value of the allowable von Mises stress for the substrate in use.

### 1.1.1. Stress distribution

The stress distribution in a bonded joint is complex and has a significant effect on the failure criteria and the maximum strength that the joint can support. The stress distribution is influenced by several factors, including the geometry of the joint, the material properties of the adhesive and the adherents, and the loading conditions. The adhesive stress is maximum (and thus failure most likely) at the overlapping end of the thinner loaded adherents [25].

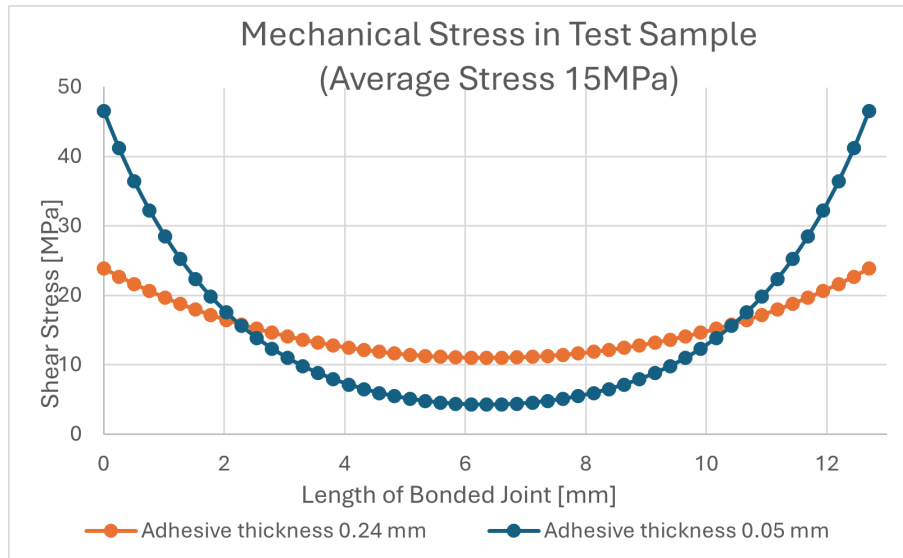


Figure 1.4: Stress distribution in adhesive length

**Influence of Material Properties** The adhesive stiffness affects the stress distribution; a lower elastic modulus in the adhesive can result in a more evident decay of stress outside the cohesive zone. Adhesive stiffness also plays an important role, with stiffer adhesives generally resulting in stronger bonds. The CTE (Coefficient of Thermal Expansion) mismatch between the adhesive and adherend will result in internal stresses. The behavior of the adhesive (brittle or ductile) affects how the stress is distributed and how the joint fails [25].

**Geometric Factors** The overlap length of the joint influences the stress distribution; increasing the overlap length distributes the load over a wider area, but this relationship is not always linear, as an excessive overlap length can reduce the average stress [11].

The thickness of the substrates affects the stress and strain in the adhesive; thicker substrates result in less longitudinal strain in the adhesive and increased bond strength. Rounding of adhesive corners reduces stress concentration and can significantly affect joint strength, especially in joints with brittle adhesives where a large radius can increase strength by 40% compared to a sharp corner.

**Maximum Strength** The maximum strength of the bonded joint does not always correlate with the maximum stress or strain values because cracks do not necessarily initiate at the location of maximum stress or strain. For brittle adhesives, failure is often dominated by stress concentrations at the corners. For ductile adhesives, failure may involve yielding and crack propagation, making predictions more complex [22]. Maximum strength is limited by the yield strength of the adhesive and the geometry of the joint. The strength

of the joint is influenced by the ability of the adhesive to deform or yield before failure, which is related to the size and shape of the stress area in the joint.

## 1.2. Substrate

The mechanical components to be bonded, according to design, are generally made of titanium or invar, while the lenses can be made of germanium or glass (fused silica). In the case of structural glass-metal bonding, the contact areas are distant from the part of the lens with optical function. In this way, any small fractures or imperfections that might form near the bonding do not directly affect the quality of the image captured by the lens. However, localized stresses in these contact areas can generate strains, which in turn could cause deformations in the lens, compromising its proper function.

Metals generally have high surface energy, which makes them easier to bond than many other materials. The adhesive must adequately wet the metal surface to ensure a strong bond. Low-viscosity adhesives can penetrate microscopic irregularities in the metal surface. Heating the adhesive can improve the flow and effectiveness of bonding. For metals, surface tension does not pose as much of a problem as for other materials such as plastics.

Metal surfaces should be thoroughly cleaned before bonding. Contaminants such as grease, oils, and oxides must be removed to ensure that the adhesive can adhere directly to the metal surface. Some adhesives, such as acrylics, can tolerate less clean surfaces, but in most cases, cleanliness is critical for optimum adhesion performance.

Primers are applied to treated surfaces to improve adhesion and protect the surface. They can dissolve contaminants, improve corrosion resistance, and provide a stable base for the adhesive. Primers are chemically reactive, making them very effective for long-term adhesion strength.

## 1.3. Type of adhesives

### 1.3.1. Optical cements

These adhesives are typically used to bond optical components such as lenses, prisms and mirrors. Optical cements must have high optical clarity and minimal light absorption to avoid interfering with the optical paths of the instrument. The most common are UV-curable and are designed to have a refractive index close to that of the optical components they bond. Examples include UV-curable acrylics and optical-grade epoxies. These adhesives provide precision bonding and excellent optical transparency, making them ideal

for applications such as telescopes, microscopes and sensors.

Curing of this type of adhesive occurs in two steps: a short exposure (typically to a UV lamp at 30.5 cm for 20 minutes) followed by a 90-minute exposure to the same lamp at the same distance. With a long-wave (wavelength 366 nm) fluorescent tube UV light source, an initial 10-minute exposure is recommended followed by a second 60-minute exposure, both at 2.5 cm. Bonded parts can be handled with care even after the first exposure. For maximum stability, the joint should be fully cured before handling.

### 1.3.2. Structural adhesives

Unlike optical cements, structural adhesives are designed for mechanical strength and durability rather than optical properties. These adhesives bond components into instruments where the primary concern is mechanical integrity rather than optical transparency. Structural adhesives, such as epoxies, polyurethanes, or silicones, are designed to withstand environmental stresses, such as thermal cycling, vibration, and mechanical loading, common in space and aerospace applications. They provide a strong bond for mounting optical assemblies or holding instrument housings together.

In opto-mechanical systems, these two classes of adhesives are chosen based on the priority of optical performance or mechanical stability. The choice of adhesive is critical to maintaining both the accuracy of optical alignment and the overall structural integrity of the instrument.

Epoxy resins are versatile thermosetting resins. They are durable, have excellent thermal and adhesive properties, and are formulated as liquid, paste, tape, film, and powder resins. Liquid and paste forms are widely available as one- or two-component types. Some can be cured at room temperature. Thermal and mechanical properties improve if polymerization occurs at temperatures up to 175°C (generally). Some types contain powdered metals or other fillers to improve their properties. For example, silver powder increases electrical conduction, aluminum dioxide improves thermal conduction, and silica powder serves as a thickening agent.

## 1.4. Adhesive selection

**Technical specifications and requirements:** the first step is to define the technical specifications of the adhesive. This includes understanding the required mechanical properties (such as strength, stiffness, and durability), surface treatment, curing mechanisms, and environmental factors. A well-defined specification helps narrow the adhesive

options and ensures that the adhesive system meets the functional requirements of the product. Also, ensure that models used for adhesive joints accurately predict stress and deformation.

**Product properties:** the properties of the adhesive itself, such as strength, stiffness, cure time, chemical resistance, and temperature tolerance, are critical. Adhesives vary greatly in terms of mechanical performance: some are more elastic, others offer greater structural stiffness. In addition, numerical models must be implemented to help predict the behavior of adhesives under different loading conditions, further aiding the selection of suitable adhesives. Factors such as adhesive thickness and ability to resist fracture propagation are critical to long-term performance. Selecting an adhesive with the right properties for the specific use case is essential.

**Low Outgassing:**  $RML < 1.0\%$  /  $TML < 0.1\%$  /  $CVCM < 0.01\%$ . Low outgassing is a key requirement for adhesives used in space applications because of the extreme vacuum environment of space. Under vacuum conditions, materials can release volatile components, which can condense on critical surfaces such as optical lenses, causing contamination and performance degradation. The European Space Agency (ESA) requires specific outgassing standards through the ECSS-Q-ST-70-02 standard, which defines the "Thermal Vacuum Outgassing Test" used to test materials for use in space. This document specifies two parameters: Total Mass Loss (TML) and Collected Volatile Condensable Material (CVCM) to ensure minimal material release in a vacuum environment. According to the ECSS standard, materials must have a TML of less than 1.0 percent and a CVCM of less than 0.1 percent to be considered suitable for space. The testing process involves subjecting material samples to elevated temperatures in a vacuum, simulating the harsh space environment, and evaluating the outgassing behavior of the material by comparing the mass before and after the test. This ensures that the adhesive will not degas or contaminate other spacecraft components during the mission.

Other factors to be taken into consideration include:

- **Thermal Stability:** Space materials must withstand extreme thermal cycles and rapid temperature changes ( $-100^{\circ}\text{C}$  to  $+150^{\circ}\text{C}$  or even more extreme values depending on the application). The adhesive must maintain mechanical and adhesive properties during and after numerous thermal cycles.
- **Resistance to Radiation:** The space environment exposes materials to ultraviolet (UV) light, ionizing rays, and high-energy particles. The adhesive must be able to maintain its properties in the presence of such radiation without degrading significantly.

- **Chemical and Mechanical Compatibility:** Adhesives must be compatible with other materials used in the space system (metals, composites, polymers, etc.) to avoid unwanted chemical reactions or weak adhesions. Long-term interactions between adhesive and substrate must be tested.
- **Durability and Reliability Over Time:** Space missions can have very long durations (from several years to decades). Adhesives must ensure consistent performance over time, even in microgravity conditions and under mechanical and thermal stress.

## 1.5. Market research

In the initial phase of operations research, a preliminary study was conducted to define the objectives and acceptable parameters for bonding intended for space use. During this phase, two types of bonding of particular interest to the company were identified: optical and mechanical surface bonding. One of the main challenges faced was bonding between metal parts and optical surfaces, as it required an adhesive compatible with both materials. Consequently, attention was focused on finding adhesives that met this specific need. Subsequently, a small database of candidate adhesives for application was compiled, that can be found in the Appendix (A.1 , A.2). During this process, special attention was paid to critical factors such as potential outgassing and adhesive shrinkage. Discarding adhesives that did not meet these requirements was a critical step in ensuring compatibility with the space environment and proper functioning of the optical surfaces. This operations research phase provided a solid basis for selecting the most suitable adhesives and helped outline the specifications needed for the subsequent analysis and testing process.

It is crucial to identify adhesives that precisely match the company's specific needs: managing a wide array of adhesives across various projects introduces significant challenges, as it necessitates maintaining multiple distinct production procedures. Furthermore, in optical applications only a minimal amount of adhesive is required, yet, these products are typically sold in standard packages that, once opened, must be stored for a maximum of six months at cryogenic temperatures according to their datasheets. This scenario poses a significant risk of adhesives with a high manufacturing cost reaching their expiry date without having been utilized, thereby resulting in the generation of waste. Consequently, it is a strategic imperative for the company to opt for an adhesive that possesses sufficient versatility to be employed across a wide range of applications. This approach will serve to streamline production processes and mitigate material wastage.

## 1.6. Finite Element Analysis

The Finite Element Method (FEM) is a benchmark numerical technique for stress and strain analysis of structural adhesive bonds. Various techniques exist to simulate the thin adhesive layers of bonded joints.

In structural adhesives characterized by high elastic modulus and small contact surfaces, phenomena such as peeling tend to be negligible. In these cases, cohesive and adhesive failure within the adhesive layer is the predominant mechanism.

Through FEM, several failure criteria can be implemented to predict the strength of the joint, including:

**Criteria based on maximum deformation.** These criteria predict failure by comparing the maximum stress or strain in the adhesive with critical values derived from experimental tests. However, they are particularly sensitive to mesh size, especially at singular points where stresses tend to infinite values. Like the Critical Longitudinal Strain (CLS) criterion. According to this criterion, joint failure occurs when the longitudinal deformation along the intermediate plane of the adhesive reaches a critical value at a certain distance from the ends of the overlap.

**Criteria based on plastic strain energy density.** Failure is predicted when the plastic strain energy density in a given area of the adhesive reaches a critical value. This approach is shown to be less influenced by mesh size than criteria based on maximum stress or strain.

**Fracture mechanics methods.** These methods focus on using the fracture toughness of the adhesive as the main parameter. However, fracture toughness can be affected by the geometry of the joint, especially in the case of adhesives characterized by ductile behavior.

**Cohesive Zone Models (CZMs).** CZMs allow the simulation of damage growth along a predefined path by specifying a tensile-separation relationship between coincident nodes located on either side of the crack path. Compared with other approaches, CZMs are less sensitive to mesh size and allow the entire process of failure and crack propagation to be analyzed [3, 11, 23, 24, 27, 28].

### 1.6.1. Finite element analysis of adhesive bonded joints using Simcenter 3D

When dealing with very strong but fragile adhesives, it's crucial to create a precise model. This helps to predict how the adhesive might break. Simcenter 3D provides an integrated

environment that simplifies the entire analysis process. This includes creating the geometry, defining the materials, creating meshes, solving the problem, and post-processing.

**Geometry Definition and Assembly:** The initial step in this process is to either create or import the joint geometry. In the majority of cases, the geometry is imported from the CAD files that are created for the production of the actual part or the sample. The geometry is simplified to have a lower impact on meshing effort in areas that are not of interest to the analysis. In practice, the geometry typically consists of the adherends (substrate materials) and the thin adhesive layer. Simcenter 3D's CAD capabilities allow the precise definition of complex joint configurations. Care must be taken to model the adhesive layer with the appropriate thickness, especially when it is very thin relative to the adherends. The approach used is to define a separate "bonding" region that can later be assigned specific adhesive properties.

**Material Property Definition:** For accurate simulation, material models must be defined for both the adherends and the adhesive. Very strong, brittle adhesives are typically modeled as linear elastic materials with a high Young's modulus and low ductility. Alternatively, if failure prediction is required, a cohesive zone model (CZM) can be implemented. In Simcenter 3D, you can assign a bilinear traction–separation law to the adhesive layer, specifying parameters such as initial stiffness, cohesive strength, and fracture energy. In our experience, using detailed experimental data to calibrate these parameters is essential for capturing the brittle failure behavior accurately.

**Contact and Bonding Definition:** One of the unique features of Simcenter 3D is its robust handling of contact and bonding. For adhesive joints, the adhesive layer can be modeled in one of two ways:

- *Cohesive Elements:* Here, the adhesive is replaced by a layer of cohesive elements that simulate the traction–separation behavior. This approach is particularly effective for capturing damage initiation and progressive failure in brittle adhesives.
- *Tie Constraints or Gluing Contact:* a tie constraint can be used to 'glue' the adherends together. However, this method does not capture the failure characteristics of the adhesive, which are known by testing and comparing the stresses in the adhesive layers.

**Boundary Conditions and Loading:** The next step is to apply appropriate boundary conditions and external loads. Typically, one end of the joint is fixed while a load (or displacement) is applied to the other. In static simulations, it is crucial to gradually increase the load to capture potential snap-through or unstable slipping phenomena.

Simcenter 3D's step-wise load application and nonlinear solution capabilities help manage convergence issues that can arise from sudden stiffness changes in the adhesive.

**Meshing Strategies:** A high-quality mesh is crucial for resolving stress gradients in the adhesive layer. Fine meshing in the adhesive layer is used to avoid over- or under-predicting stress concentrations. Simcenter 3D provides advanced meshing tools that allow for structured or free meshing depending on the geometry's complexity. For adhesive joints, a finer mesh is typically applied in the adhesive layer and in the vicinity of the bond. We often use solid elements (e.g., hexahedral or tetrahedral elements) for the adherends and specialized elements for the adhesive. Mesh refinement studies are recommended to ensure the convergence of stress results without introducing numerical artifacts.

**Solver Settings and Nonlinear Analysis:** When modelling adhesive bonded joints with brittle adhesives, nonlinear behavior is often encountered due to damage evolution. Simcenter 3D's solver can handle nonlinear static and transient analyses, and careful attention should be given to the solution controls. Adjustments such as load increments, convergence criteria, and viscous regularization may be necessary. Our experience suggests that starting with a linear analysis to validate the model and then gradually introducing nonlinear material behavior often leads to more stable and reliable solutions.

**Post-Processing and Results Extraction:** After the solution has been obtained, Simcenter 3D offers a suite of post-processing tools to extract and visualize the results. Key outputs include:

- *Stress and Strain Distributions:* Detailed contour plots of von Mises stresses, normal and shear stresses in the adhesive and adherends.
- *Damage Indicators:* For cohesive models, parameters such as damage initiation and progression (often represented as a scalar degradation factor) can be plotted.
- *Load-Displacement Curves:* These curves provide insight into the joint's stiffness and failure load.

In practice, we typically export these results to both graphical formats for visual inspection and numerical formats for further statistical analysis or validation against experimental data. Careful interpretation is necessary to differentiate between numerical inaccuracies and true physical behavior.

### 1.6.2. Cohesive elements and their limitations

Cohesive zone modeling (CZM) has emerged as one of the most popular numerical approaches for simulating damage and failure in adhesively bonded joints. By representing the adhesive layer with cohesive elements governed by a traction–separation law, CZM captures the progressive degradation of the bond. These elements’ ability to simulate damage growth, predict strength, and analyze the influence of geometric parameters makes them particularly suitable for the design and optimization of bonded joints.

Many sources reviewed highlight several cases in which the use of a model with cohesive elements can be advantageous for the study and analysis of stress in bonding:

*Modelling damage growth:* Cohesive zone models (CZMs) are particularly suitable for simulating damage growth in bonded joints. Unlike traditional methods based on tension/deformation criteria, CZMs allow the initiation and propagation of fracture to be modeled more realistically, taking into account the ductility of the adhesive and its ability to transfer loads even after damage initiation [3, 23].

*Strength prediction:* CZMs make it possible to predict the strength of bonded joints under different loading conditions. Using tensile-separation laws, the behavior of the adhesive up to failure can be simulated, resulting in an estimate of the maximum load that the joint can withstand. This is particularly useful in the design of bonded joints, as it allows the geometry and adhesive selection to be optimized to achieve the desired strength [2].

*Study of the influence of geometric parameters:* CZMs allow the evaluation of the effect of geometric parameters, such as overlap length and shape changes, on the strength of the bonded joint. This is useful for optimizing the geometry of the joint according to the applied stresses and adhesive properties.

*Analysis of different adhesive types:* CZMs can be used to model the behavior of different adhesive types, from brittle to ductile. The ability to define specific tensile-separation laws for each adhesive allows their mechanical behavior to be accurately simulated and the strength of the bonded joint to be predicted as a function of the properties of the adhesive used [3].

## Limitations

The effectiveness of Cohesive elements is critically dependent on the precise characterization of the adhesive’s mechanical behavior. Several major limitations remain. In particular, when dealing with very strong and brittle adhesives, obtaining reliable parameters for the cohesive law requires highly specialized tests that demand both sophisticated

equipment and an exceptional level of precision.

### **Challenges in Cohesive Element Calibration**

The accuracy of cohesive element models hinges on the calibration of the traction–separation relationship. This calibration involves determining key parameters such as the initial stiffness, cohesive strength, and fracture energy from experiments. Standard tests like the Double Cantilever Beam (DCB), T-peel, or Single Lap Joint (SLJ) tests are employed to characterize these properties. However, for very strong and brittle adhesives, the process zone is extremely narrow, which makes the measurement of minute crack opening displacements and stress levels particularly challenging. The required experimental setups must possess exceptional resolution and control, often involving laser-based measurement systems or high-precision load frames, equipment that is both costly and not widely available. Moreover, cohesive properties, such as strength and fracture energy, often depend on the thickness of the adhesive. This dependence requires characterization of the cohesive law for a range of application-relevant thicknesses, increasing the experimental effort [12].

### **Limitations in Representing Non-Cohesive Damage**

While cohesive elements are designed to simulate the gradual degradation and eventual failure of the adhesive material itself (i.e., cohesive failure), they are less effective when the dominant failure mode is adhesive failure. Adhesive failure occurs when the bond between the adhesive and the substrate is compromised, a mechanism that involves complex interfacial phenomena such as surface roughness, chemical bonding, and microscopic defects. The prevailing CZM framework operates under the assumption of a homogeneous adhesive behavior, thus inherently lacking the capacity to capture localized debonding at the interface. This limitation becomes particularly evident when the test data indicates a mixed-mode failure or when the failure originates predominantly from the adhesive–adherend interface as opposed to within the adhesive layer itself. This is the case in the majority of the studied cases, where strong adhesives were found to be capable of withstanding the stress, yet the joint failed due to adhesive failure.

### **Experimental Difficulties and Model Sensitivity**

The sensitivity of cohesive element models to calibrated parameters further exacerbates these limitations. Minor inaccuracies in the measured crack opening displacement or load can lead to significant discrepancies in the predicted failure behavior. This effect is particularly pronounced in the case of brittle adhesives, where the adhesive exhibits minimal plastic deformation before fracture. Furthermore, the equipment necessary to conduct such meticulous tests (typically incorporating high-speed data acquisition systems

and precise displacement sensors) is not only costly but also requires a level of operator expertise that may not be readily available in all research or industrial settings [4].

In consideration of the issues identified, a conventional approach was predominantly adopted, as previously outlined, incorporating three-dimensional elements and quantifying the measured stress on the adhesive. However, these challenges remain an active area of research, imperative for enhancing the reliability of finite element analyses of bonded joints.

## 2 | Projects and simulations

The purpose of the present analysis is to assess the capabilities of materials in space. At this time, it is imperative to maximize engineering efficiency in the sector of space telescopes. Some of the analyses presented in this thesis are based on projects involving constellations of satellites, such as the ESA IRIDE space program, an earth observation program based on a constellation of satellites in low earth orbit and structures on the ground. The primary objectives of this program encompass a wide range of functions, including but not limited to: marine and coastal monitoring, air quality assessment, land movement monitoring, land cover analysis, hydro weather climate monitoring, water resources monitoring, emergency management, and security.

For space applications, adhesive validation relies on a twofold strategy that combines simulation with experimental testing. First, numerical simulations are performed using datasheet values to predict adhesive behavior under expected operating conditions. However, datasheets typically report tensile and shear strengths for standard substrate pairs (usually aluminum-to-aluminum) which differ significantly from the bonding scenarios encountered in space hardware. For example, when bonding glass or germanium to titanium, factors such as surface roughness, chemical composition, and the type of primer used can substantially influence the adhesive performance. Consequently, it is necessary to conduct custom experimental tests to determine the actual bond strength between these dissimilar materials. Since brittle substrates like glass and germanium cannot be machined into standard lap shear specimens without risking damage, specially designed test fixtures are required. These bespoke specimens allow for an accurate evaluation of the adhesive force under conditions that mimic the in-service environment, thereby establishing reliable design allowables. This rigorous validation process is essential to ensure that the adhesive will perform as expected in the demanding conditions of space.

## 2.1. Effects of the space environment on substrates and adhesives

In the space environment, materials and bonding agents are subjected to extreme conditions that can profoundly impact their mechanical and physical properties. This section explores the repercussions of the space environment on metal structures, along with structural adhesives, particularly two-part epoxy adhesives employed to bond titanium or Invar structures to optical components such as glass or germanium lenses. This discussion covers the degradation of material properties, alterations in shape and volume, and the consequent impact on the life expectancy of these materials in space.

### 2.1.1. Effect of the space environment on Titanium and Invar structures

Titanium and Invar are extensively utilized in aerospace applications due to their advantageous strength-to-weight ratios and, in the case of Invar, its near-zero thermal expansion. However, the space environment imposes several challenges.

Titanium exhibits excellent mechanical properties and corrosion resistance. However, in low Earth orbit (LEO), it is susceptible to erosion from atomic oxygen. Prolonged exposure to high-energy particles and ultraviolet (UV) radiation can also lead to surface degradation and embrittlement, affecting its fatigue life and overall structural integrity [7].

Invar is prized for its low coefficient of thermal expansion (CTE), which is critical in applications requiring high dimensional stability. Despite this, Invar structures can experience slight oxidation and radiation-induced defects over extended periods in space. Additionally, micro-meteoroid impacts and thermal cycling can contribute to fatigue, necessitating careful design and protective measures [9].

### 2.1.2. Effect of the space environment on structural adhesives

Structural adhesives in space applications, such as two-part epoxies, silicone adhesives, and UV-curable adhesives, are used to bond metallic substrates (titanium or invar) to optical elements (glass or germanium). These adhesives must endure not only mechanical loads but also the unique challenges posed by the space environment:

- **Thermal and Mechanical Stress:**

Space structures are subject to extreme thermal cycling, with temperature variations that can range from  $-150\text{ }^{\circ}\text{C}$  to over  $150\text{ }^{\circ}\text{C}$ . Two-part epoxy adhesives, for instance, can experience significant changes in their tensile modulus and other mechanical properties when exposed to such extremes. Differential thermal expansion coefficients between the adhesive and its substrates often result in residual stresses, which may lead to micro-deformations, volumetric changes, and even bond failure [7].

- **Outgassing and Chemical Stability:**

In a vacuum, volatile components in adhesives may outgas, leading to material degradation and potential contamination of sensitive optical surfaces. Although silicone adhesives and UV-curable adhesives typically have lower outgassing rates, even minor losses can impact the long-term reliability of the bond.

- **Radiation Effects:**

High-energy radiation in space can induce polymer chain scission or cross-linking, altering the adhesive's properties over time. This radiation-induced degradation can reduce the adhesive's toughness and ductility, which is particularly critical for two-part epoxies that are expected to maintain their bond under load [7].

- **Life Expectancy and Reliability:**

The combined effects of thermal cycling, outgassing, and radiation lead to a gradual loss in adhesive performance. This degradation manifests as a reduction in mechanical strength and an increase in brittleness, thereby limiting the service life of the adhesive bond. Life expectancy predictions for adhesives in space must account for these factors. They often use accelerated aging tests and finite element simulations to estimate performance over the expected mission duration [5].

## 2.2. Thermoelastic analysis

Thermoelastic analysis is essential to verify the proper functioning of an instrument consisting of different components with different materials having different coefficients of thermal expansion.

The use of thermoelastic analysis makes it possible to:

- Predict and minimize the thermal stresses that develop in a joint during its manufacture and service life. Thermal stresses can result from several sources: differential thermal expansion of the adhesive and adherents and temperature gradients within

the joint. These stresses can reduce the strength of the joint and lead to premature failure.

- Understand how the properties of an adhesive change with temperature. The modulus of elasticity, strength and toughness of an adhesive can be affected by temperature. This information is important in selecting an adhesive that performs well over the expected temperature range for the joint.
- Optimize the curing process of adhesive. Temperature and curing time can influence the development of residual stress in the joint. Thermal analysis can be used to determine curing conditions that minimize these stresses.

Once assessed the structural adhesives are suited for an application is possible to analyze their behavior in the context of a project involving more complex geometries

### 2.3. Deformation of telescope lens

An additional problem related to the use of adhesives is the volume change that happens due to shrinkage during the curing process or a different coefficient of thermal expansion (CTE) with the substrate. The problem of volume change of the adhesive in optical applications, such as in the case of a telescope lens, can actually lead to residual stresses and unwanted deformation of the lens itself, which manifest as optical aberrations. Polymerization causes shrinkage of the adhesive, which is applied at specific points (six glue spots in our case). This results in a non-uniform distribution of forces on the lens. The same thing happens when a temperature load is applied, considering that the support of the lens made of Titanium or invar has a low CTE, but not as low as the HPFS glass.

During the assembly stage, adhesive is injected directly into the fitting points through small channels, and then the lens is aligned before polymerization begins. Residual stresses generated during polymerization cause microdeformation on the lens, and consequently aberrations.

The following effects occur during polymerization and subsequent adhesive shrinkage:

- Local deformations: The adhesive spots that bind the lens undergo contraction, exerting forces on the contact points between the lens and the housing (barrel). This contraction causes uneven stresses on the lens, as each bonding spot is subject to a different combination of forces.
- Rigid constraints: If the lens is fully constrained through the six adhesive points, it does not have the ability to move to compensate for the forces generated by the shrinkage of

the adhesive. This generates internal residual stresses that deform the lens surface.

- Microdeformation: The deformations that develop in the lens are not uniformly distributed, but tend to be concentrated at the adhesive spots. These localized deformations distort the wavefront of light passing through the lens, compromising optical performance.

Optical aberrations represent deviations from the ideal image that occur when an optical system, such as a lens, fails to focus light perfectly. These errors, which take the form of image blurring or distortion, are influenced by the geometry of optical surfaces.

The main aberrations that could result from this type of stress include:

1. Astigmatism: Adhesive spots cause non-uniform shrinkage along perpendicular axes, the lens may undergo elliptical deformation, leading to astigmatism. Astigmatism causes light to focus in different planes in different directions, resulting in elongated or blurred images.
2. Coma: If the deformations are asymmetrical with respect to the optical axis, the resulting aberration could be coma, which distorts the image into a "comet" shape, with a tail extending away from the center.
3. Spherical aberration: If the contraction of the adhesive is symmetrical with respect to the center of the lens, it could induce spherical aberration, in which light rays from the peripheries of the lens are focused closer than the central rays.
4. Trefoil (trefoil): The use of six adhesive spots symmetrically distributed around the lens can generate trefoil (triple symmetry) type aberrations, with a distortion of the lens shape reflected in a tripolar distribution of optical defects.
5. Tilt and decentration: If polymerization takes place unevenly or if the lens is shifted slightly during alignment, tilting (tilt) or decentration of the lens may occur, shifting the image laterally.

The use of Zernike polynomials allows these aberrations to be modeled and quantified accurately, making it easier to identify sources of deformation and allowing corrections to be made to both the design of the bonding system and the curing process.

The following optical results (2.1, 2.2, 2.3) are derived from the thermoelastic analysis of an assembly of a telescope, as detailed in Chapter 4.2. The glass lens is attached to a metal support and is supported with a silicone adhesive. The deformation of the lens surfaces is extracted from the FEA software, and the Zernike polynomials are calculated with a dedicated program.

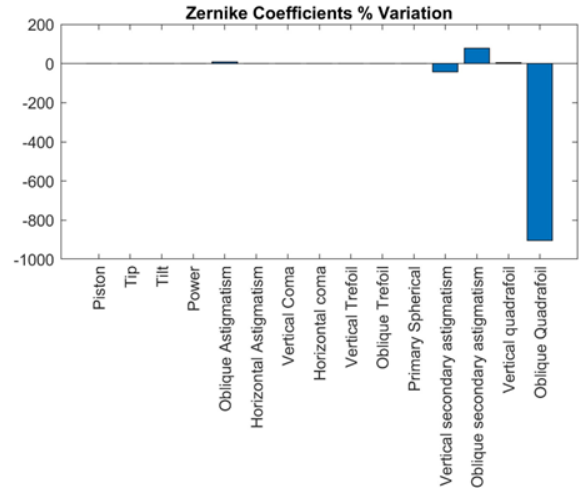
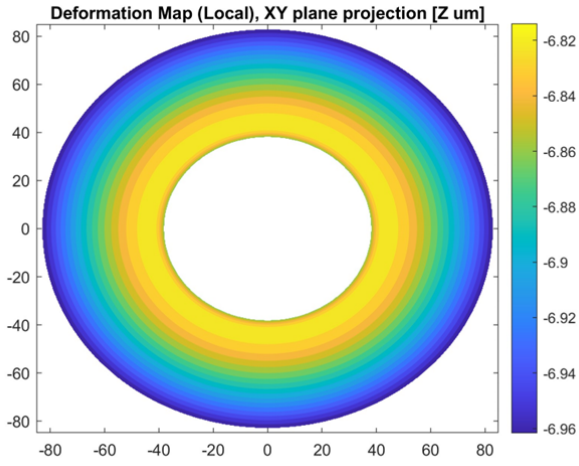


Figure 2.1: Zernike deformation map

Figure 2.2: Zernike coefficients variation

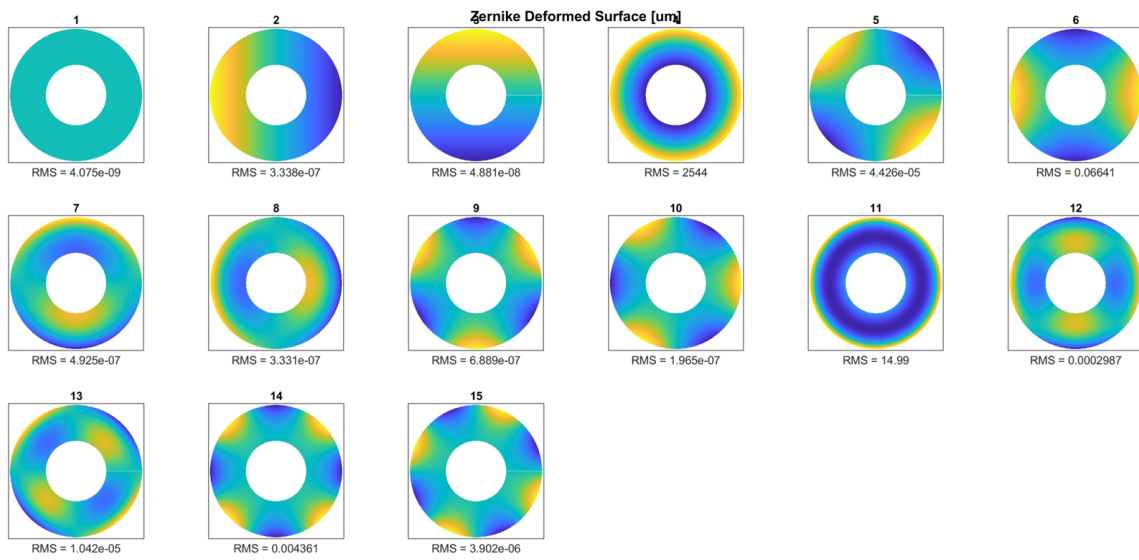


Figure 2.3: Zernike deformed surface

# 3 | Structural adhesives

There are several structural adhesives suitable for bonding substrates made of titanium, glass, or germanium. Following a market analysis, two epoxy adhesives (EP42HT-2LTE and EC2216) emerged as the optimal candidates for our design requirements. Their critical properties are summarized in the datasheets provided in the Appendix, highlighting values essential to our analysis. Both adhesives have demonstrated adequate performance for structural bonding projects; however, subtle differences in their physical properties and operational characteristics necessitate a careful, project-specific selection process.

| Name                        | EC 2216 B/A Gray       | EP42HT-2LTE                |
|-----------------------------|------------------------|----------------------------|
| <b>Supplier</b>             | 3M                     | Masterbond                 |
| <b>Temperature range</b>    | -50 a 80 °C            | -51 a 149 °C               |
| <b>Curing time at 25°C</b>  | 7 d                    | 7 d                        |
| <b>Curing time at 70 °C</b> | 2 h                    | 3 h                        |
| <b>Viscosity</b>            | Moderately fluid paste | Moderately fluid paste     |
| <b>Pot life</b>             | 90 min                 | 60 min                     |
| <b>Tensile strength</b>     | 22 Mpa                 | 41 Mpa                     |
| <b>Shear strngth</b>        | 6 Mpa                  | 5 Mpa                      |
| <b>TML</b>                  | 0.77%                  | <0.1%                      |
| <b>CVCM</b>                 | 0.04%                  | <0.01%                     |
| <b>CTE [ppm/°C]</b>         | $45 \times 10^{-6}$    | $9 \div 12 \times 10^{-6}$ |

Table 3.1: Structural adhesives examined

## 3.1. EC2216

Inside the company, the EC2216 epoxy adhesive is routinely used to bond optical components (such as lenses) to the assembly's housing (commonly referred to as the barrel). Its selection is based on a proven record of performance with substrates like titanium, glass, and germanium. However, when deploying EC2216 in new applications that involve substrates not covered in the standard datasheet, it is essential to perform additional tests and simulations to establish reliable design allowables. For instance, a specific lap shear test studied for the case is necessary to evaluate the adhesive force between germanium and ti-

tanium. Such tests are challenging because they require high-precision instrumentation to accurately capture the very narrow process zone typical of strong, brittle adhesives. This rigorous experimental approach ensures that the adhesive's performance is fully characterized under the new bonding conditions, thereby enabling safe and effective application in advanced optical assemblies.

### 3.1.1. Tensile test

In the development of advanced adhesive bonding solutions for critical applications, it is essential to validate the performance of the adhesive both under standard operating conditions and after exposure to environmental stressors such as thermal cycling. Rigorous testing not only ensures that the adhesive meets the design allowables but also highlights the importance of quality control in the manufacturing process. The following section summarizes the outcomes of our comprehensive testing protocol, which included tensile evaluations and thermal cycling tests.

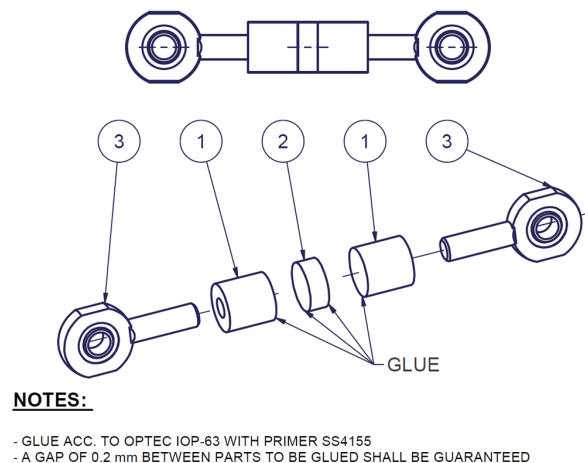


Figure 3.1: Tensile test specimen

**Test Results and Conclusions** The same specimen configuration was used for a variety of substrates with only minimal modifications. This specific geometry was dictated by the inability to directly connect one component of the substrate to the traction machine. Tests were carried out on two substrate combinations:

1. Titanium-Germanium
2. SuperInvar-Fused Silica

Based on the tests conducted, the following conclusions regarding adhesive performance were reached:

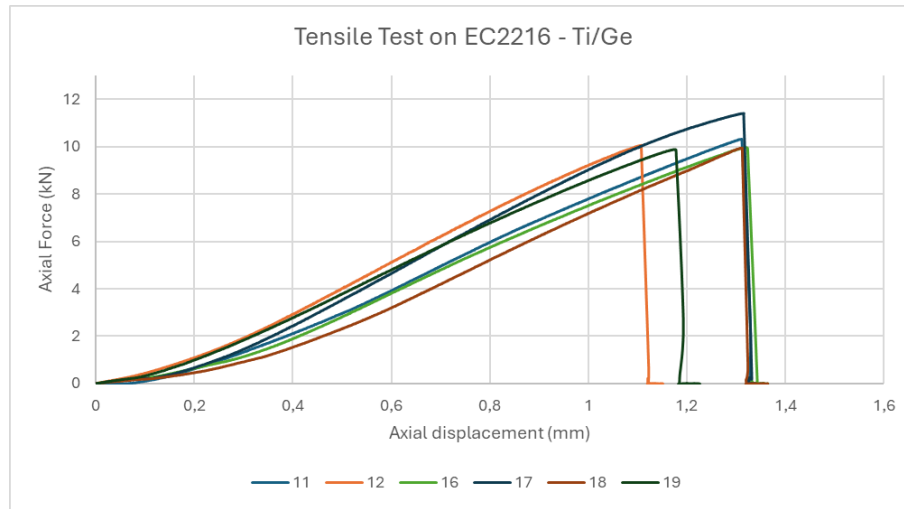


Figure 3.2: Tensile test results. Mean value: 20 MPa; Standard Dev.: 0.97 MPa

**Titanium-Germanium:** All specimens, including those that underwent thermal cycling, successfully passed the test. The average von Mises stress recorded in the adhesive was 20 MPa, with no sample falling below 18 MPa. This performance exceeds the acceptance criterion, which requires that the stress must be greater than 15.9 MPa plus a 10% degradation allowance (i.e., 17.2 MPa). The standard deviation is 0.97 MPa; however, excluding faulty specimens is 0.72 MPa.

The average measured stress is only slightly lower than the maximum value of 22 MPa reported in the adhesive datasheet for aluminum-to-aluminum bonding scenarios. This indicates that, even under varied conditions, the adhesive performs reliably near its expected maximum strength.

#### Reliability and Quality Control:

A few samples were rejected due to manufacturing errors that adversely affected their mechanical behavior. In particular, errors in achieving the specified adhesive thickness (intended to be maintained by two 0.25 mm filaments) resulted in deviations that were not representative of the adhesive's true performance. Overall, the specimens that met the design specifications demonstrated a strength capacity well above the minimum requirement, confirming the adhesive's validity both under normal conditions and after thermal cycling. These findings underscore the critical importance of stringent quality control over production parameters, such as adhesive thickness, to ensure consistent and reliable performance.

**Superinvar-Fused Silica:** Using the same specimen geometry as before, we evaluated the adhesion of Super Invar and Fused Silica (glass) for lens applications. In this study,

surface preparation was optimized to achieve the necessary surface roughness for improved adhesion. As illustrated in the figure 3.3, specimens with abraded surfaces exhibited excellent stress performance that even exceeded the datasheet values. For the metal surfaces, the first test employed manual scratching to introduce roughness, while the second and third tests utilized abrasive paper. Although these methods rely heavily on operator repeatability, similar results can be achieved through automated processes through a machine. For the glass surfaces, manual scratching was performed in the first two tests, and a laser tool was used in the third test to regulate surface roughness. The performance increase of the specimens with surface treatment in 3.3 is by 72% compared the case without surface treatment and 21% compared with only the metal treated.

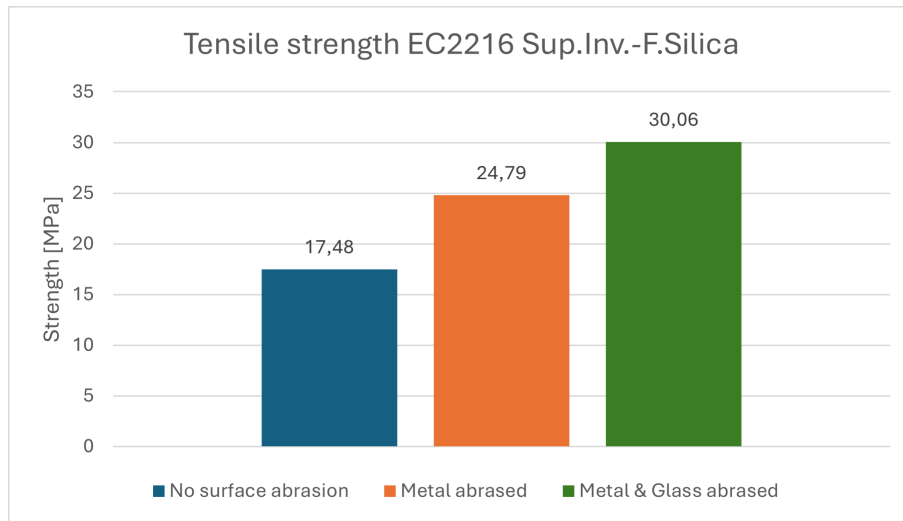


Figure 3.3: Difference in tensile performance for different surface roughness.

#### Surface roughness

| Metal            | Tool               | Glass            | Tool               |
|------------------|--------------------|------------------|--------------------|
| $< 1\mu m$       | Manually scratched | $ca.1\mu m$      | Manually scratched |
| $1.5 - 1.9\mu m$ | Abrasive paper     | $3.0 - 4.5\mu m$ | Laser              |

Another important consideration is the curing process of the adhesive. According to the datasheet, the adhesive can be cured by resting for 7 days at room temperature or for several hours (overnight) at 70 °C. Comparative testing indicates that curing at high temperatures (in an oven) results in superior adhesive performance compared to room-temperature curing with a strength improvement of 17% (figure 3.4). In practical applications, it is crucial to verify that any machinery or components in contact with the adhesive can tolerate the high-temperature curing cycle. It is also worth noting that surface roughness plays a much more significant role in determining adhesive strength than the curing temperature.

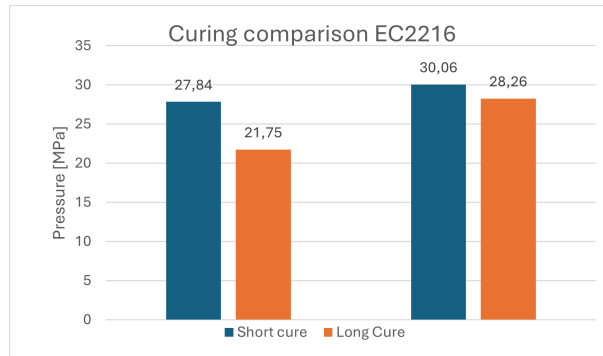
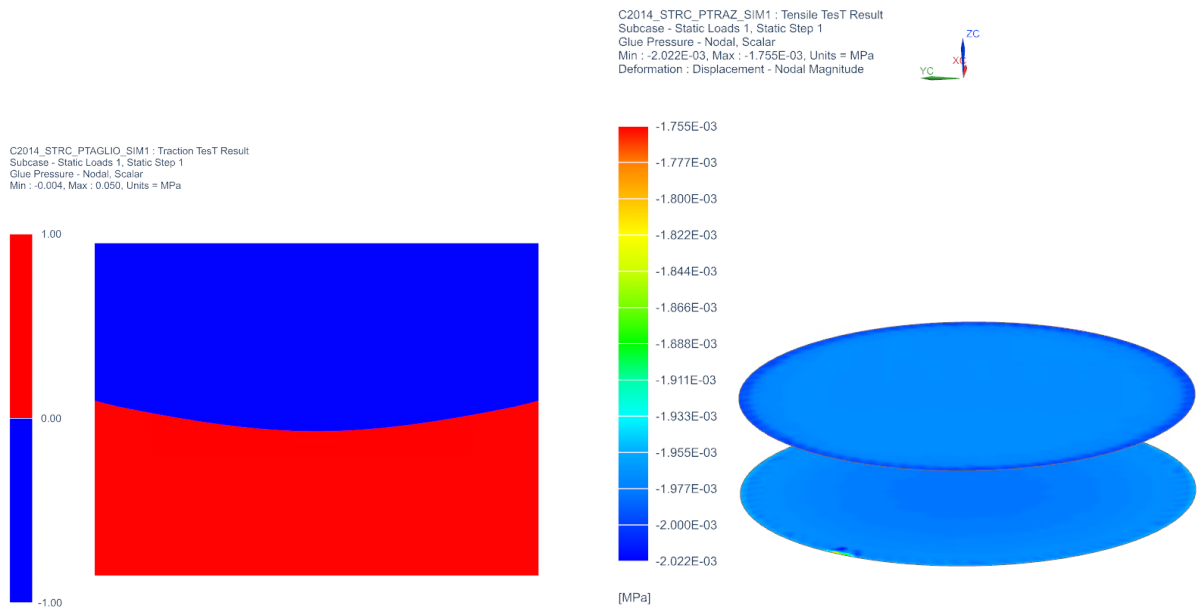


Figure 3.4: Strength of different curing process. Left: Metal abraded; Right: Both abraded

### Results analysis

An analysis was performed to compare experimental test results with finite element models in order to determine the maximum allowable stress in the adhesive layer. The stress distribution within the adhesive was examined in detail, allowing us to benchmark the applied loads from simulated cases against this new allowable limit. By comparing the simulated load conditions with the established allowable stress, it is possible to calculate a margin of safety that confirms whether the adhesive bond remains within safe operating limits. This approach is essential for ensuring that the adhesive will reliably perform under expected service conditions and for identifying any potential risk of premature failure.



(a) Stress distribution in the adhesive layer

(b) Adhesive layer simulation

Figure 3.5: Stress distribution model of adhesive layer

### 3.1.2. Shear test

In this experiment, the adhesive was evaluated in two distinct scenarios: Titanium-Germanium and SuperInvar-Fused Silica bonds. However, the shear specimens utilized in this study differed from each other. The objective of both shear specimens is to minimize the coupling between shear and bending; Nevertheless, the fragility of the substate must be taken into consideration.

## Titanium-Germanium

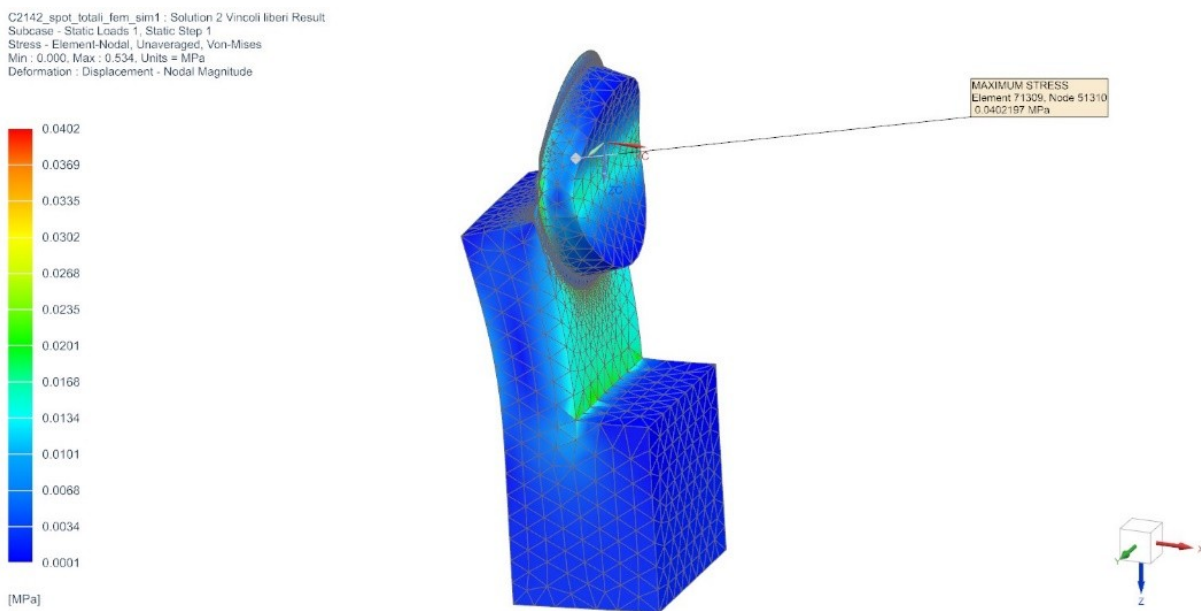


Figure 3.6: Shear test simulation model

This test aims to evaluate the structural integrity of a germanium lens fixed to a cylindrical structure. As mentioned, the specimen has a special geometry to allow the shear phenomenon to be observed without directly connecting the germanium part to the testing machine. The adhesive is applied through channels, forming a circular adhesive spot with a diameter of 8 mm. (Figure 3.9b) The size of the adhesive dot is adjusted through a second channel, positioned 4 mm away, allowing observation during application. The thickness of the adhesive dot is 0.25 mm.

From the tests conducted, it was possible to identify a limit value with acceptable data dispersion. Although rupture occurs systematically in the substrate (germanium), the stress values calculated in the adhesive at the rupture load appear to be at the limit of acceptability. Nevertheless, the test specimen was fabricated in a manner divergent from the prescribed project, thereby conferring an adhesive surface area of increased dimensions

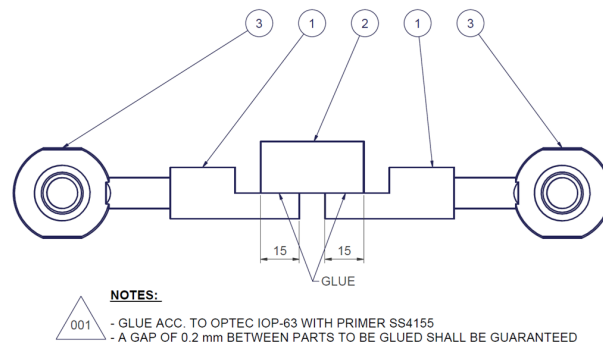


Figure 3.7: Shear test specimen

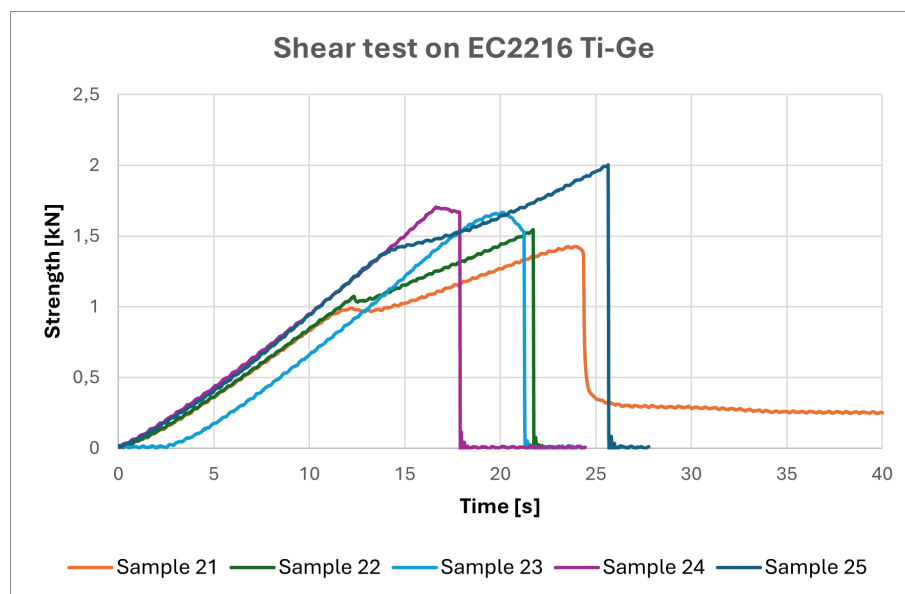


Figure 3.8: Shear test results

that can withstand a greater load (Figure 3.10a). This results in the germanium substrate undergoing failure prior to the adhesive.

The behavior of the adhesive-substrate system is at the limit of acceptability. If necessary, further modifications to the specimen geometry or adhesive (e.g., increased ductility) could provide a wider margin of safety, reducing the risk of failure in operational applications.

The findings of this test indicate that the minimum stress level at which the adhesive can withstand failure is 7.1 MPa, with a dispersion rate of 17% and a standard deviation of 0.82 MPa. This result is considered acceptable and exceeds the acceptable values calculated for the primary project design.

**Simulation:** From the original specimen, two model configurations were developed: one version represents the adhesive dot as a simple disc, while the other depicts the adhesive

dot as a disc with an additional cylinder (which corresponds to the adhesive channel). The objective of this study is to ascertain whether the simplification of the geometry of the adhesive spot in the analysis will result in substantial changes to the material representation. To evaluate the influence of the constraint representation, simulations were performed using different types of constraints. The results indicate that representing the actual constraints by representing the entire geometry of the adhesive does not yield significant differences in the stress distribution (as shown in the figure 3.9 (b)).

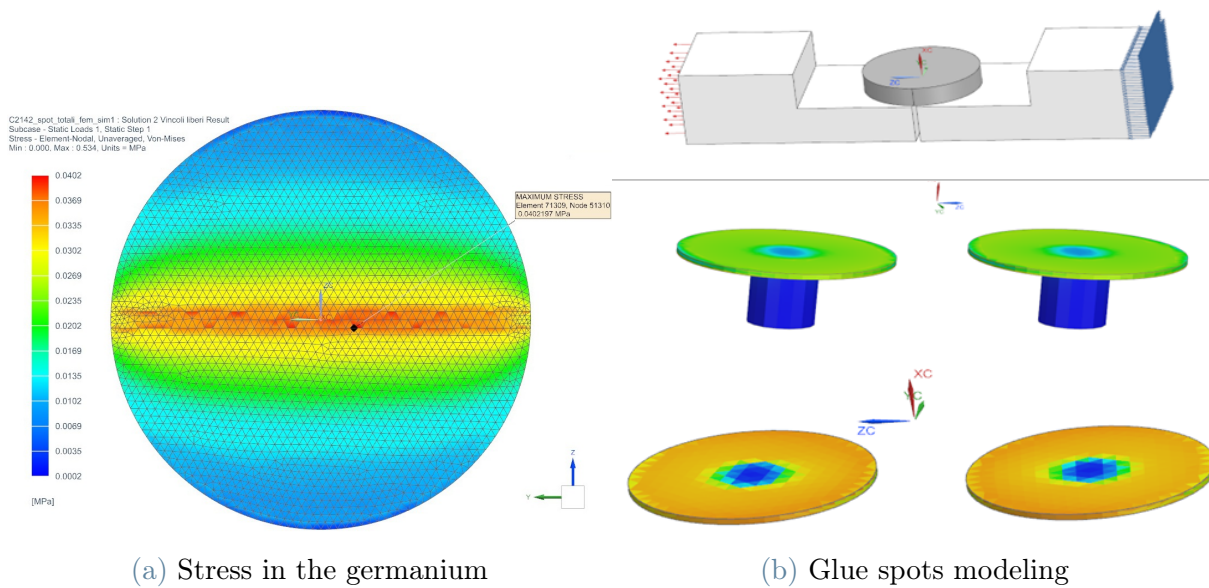


Figure 3.9: Shear test simulation

The simulation data lead to the following conclusions:

- The presence or absence of the adhesive cylinder below the adhesion point does not significantly affect the stresses recorded at the critical location. Therefore, it is advisable to adopt the simplest geometry (thus reducing computational costs), especially in complex models.
- The peak stress is located near the adhesive passage hole; however, this value can be neglected because the maximum stress is consistently found at the edges of the adhesion point.

Further simulations are necessary to investigate the various issues that were identified during the testing phase:

The simulated specimens do not achieve a state of pure tension but consistently exhibit bending moments that alter the results. This effect, particularly critical in shear tests,

is due to the geometry of the pull-out specimen. The configuration of the specimen introduces inherent bending moments. The cause of this is the germanium component that cannot be directly connected to the draw rod. Therefore, an intermediate metal support with gripping mechanisms is required. This arrangement generates multiaxial stresses at critical points, as revealed by FEM analysis. The von Mises stress calculated at these points is considerably higher than the simple shear stress predicted using the theoretical formula ( $\tau = F/A$ ).

The surface area of the bonded region is excessive. The configuration with the larger adhesive area (Figure 3.10a) results in premature germanium failure before the adhesive failure. This outcome is attributable to the combination of bending and multiaxial stresses acting on the specimen.

During specimen preparation, the entire available surface was mistakenly bonded, rather than adhering to the smaller area specified by the original design. The error in question led to an increase in the adhesive's resistance, resulting in a high stress concentration at the center of the germanium disc. In this new case, the glue spot is a semicircle with a radius of 12.7 mm, compared to the originally planned spot of 8 mm radius. A comparison of the stresses between the two configurations shows that the region with the larger radius experiences significantly lower stress than the region with the smaller radius under the same load. It is therefore reasonable to assume that, in the case of the smaller adhesive spot, the adhesive reached failure before the germanium did (Figure 3.10).

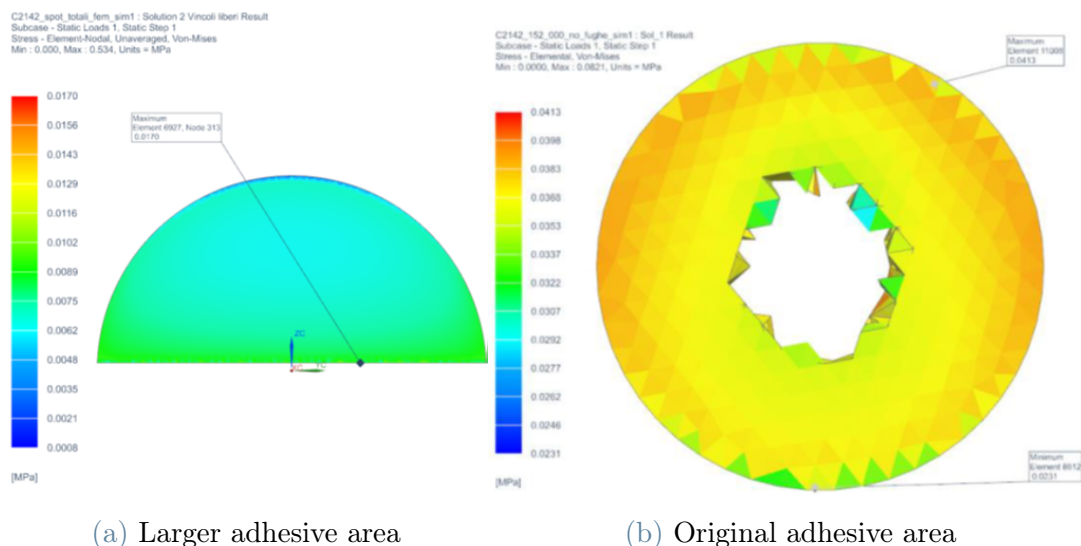


Figure 3.10: Shear test simulation of the two adhesive areas configurations

For the configuration with the larger adhesive spot (Figure 3.10a), FEM results indicate a maximum stress in the adhesive of 0.021 MPa for a 1 N force, concentrated in a very

small area at the time of germanium failure. For the original geometry (Figure 3.10b), CTETRA10 tetrahedral elements were employed. The CTETRA10 element is a 10-node quadratic tetrahedron (comprising 4 corner nodes and 6 mid-edge nodes) which allows for greater accuracy than the simpler linear CTETRA4 element. Due to its quadratic shape functions, the CTETRA10 element is particularly effective at capturing complex stress distributions in irregular geometries or regions with significant curvature. It is widely used in structural, thermal, and multiphysics simulations, offering improved accuracy in areas with complex geometric details, although this enhanced accuracy comes at the cost of increased computational effort.

**Model Convergence:** A convergence study was conducted for this model, employing CHEXA elements. CHEXA8 elements are three-dimensional hexahedral finite elements with eight angular nodes, each of which has three translational degrees of freedom. These elements employ linear shape functions, rendering them well-suited for the modeling of volumetric regions within structured meshes. The efficacy of CHEXA8 elements in structural and thermal analyses stems from their capacity to provide precise stress and displacement outcomes in regular geometries while minimizing computational demands.

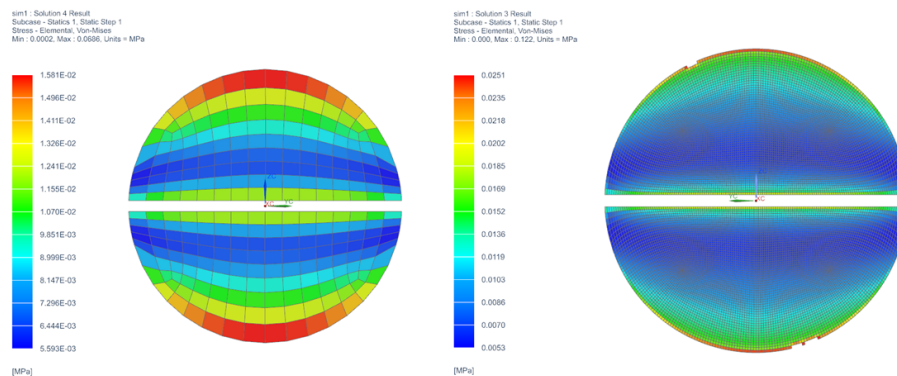


Figure 3.11: FE Models of adhesive spot

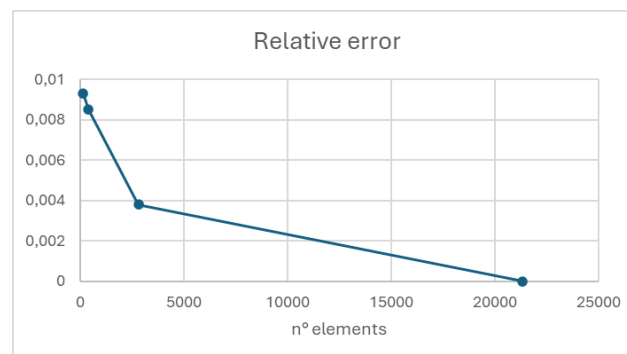


Figure 3.12: Convergence vs. n° of elements

**Validation of cohesive elements:** By using a nonlinear-MULTISTEP analysis in Simcenter 3D, an attempt to validate cohesive elements was made as a method to simulate adhesive behavior even in the absence of complete material characterization data. In this study, MATCZ and PSOLCZ material models were employed to define the constitutive tensile-separation relationship of the cohesive elements. Preset parameters for fracture initiation and propagation were used for a hypothetical adhesive that is more ductile than the EC2216 adhesive previously tested. The simulation results indicated that the maximum stress at the critical point (near the adhesive/channel interface) was 0.017 MPa. Although this value is slightly lower than those obtained with structured quadratic tetrahedral elements, the discrepancy is minimal, which suggests that cohesive elements can yield predictions even without fully characterized parameters. Key issues identified in the analysis include singularities at the interface between the adhesive channel and the adhesion point (the mesh resolution was insufficient to capture the detailed behavior). A comparison with structured elements is recommended. The use of CTETRA10 quadratic tetrahedral elements provided a satisfactory approximation even with moderately refined meshes. Moreover, further mesh refinement does not impose prohibitive computational costs; therefore, for more accurate results, it is advisable to employ a finer mesh. However, it is important to note that incorporating fracture mechanics into cohesive element simulations considerably increases the computational cost, making this approach less convenient for routine analyses.

In conclusion, while cohesive elements are an alternative to structured quadratic tetrahedral elements for modeling strong and brittle adhesives, they are less accurate and more computationally expensive. For advanced simulations, such as those that involve fracture propagation, cohesive elements remain indispensable provided comprehensive material characterization data. The observed discrepancies underscore the necessity of using a properly refined mesh to minimize the impact of singularities and to ensure reliable analysis without increasing computational expenses.

### SuperInvar-Fused Silica:

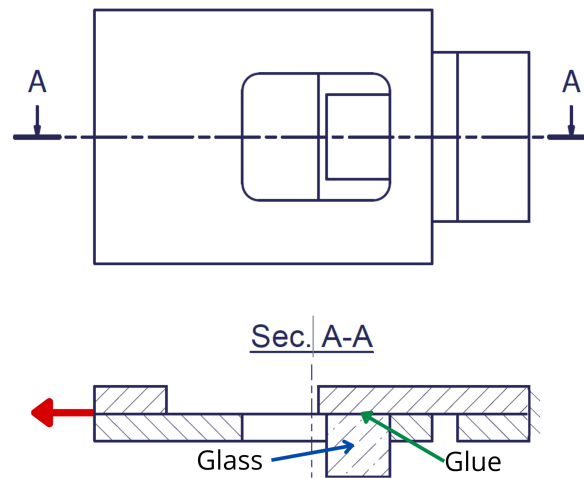


Figure 3.13: Shear test specimen

In this case, the surface roughness of the substrate was examined to assess its impact on performance, as was previously done in the tensile test. The minimum recorded value is 8.9 MPa, indicating a margin for the application of adhesives in flight projects. When both surfaces are prepared for adhesion with roughness of the surface, the strength increases by 29%.

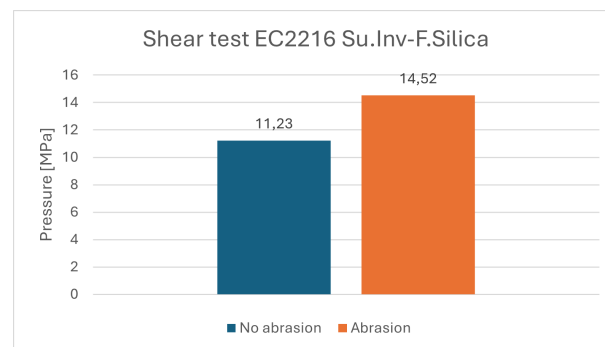


Figure 3.14: Difference in shear performance for different surface roughness

#### 3.1.3. Static test on a lens in its barrel

Due to a fault with the lens of a telescope assembly, we had the opportunity to test and run a simulation on a lens in its barrel. The test was a simple compression test to verify the shear strength of the bonded joint of the lens.

To assess the performance of the EC2216 adhesive in a real application, specimen tests were conducted on a lens assembly. In this design: the lens is secured by seven spots of

EC2216 epoxy, with additional Nusil CV2216 glue spots applied around the perimeter to cushion shocks and maintain alignment.

**Operating conditions and observations:** A force is applied along the z-axis (from top to bottom), creating specific stress distributions due to the assembly's geometry. The curvature of the lens leads to uneven stress distribution: compressive stresses are transferred to the surrounding barrel, while shear stresses concentrate at the adhesive spots (although with reduced intensity because of the lens shape). This geometry increases the force required for detachment compared to a flat-surface configuration. The combined shear and compressive stresses produce a more favorable adhesive behavior, thereby reducing the likelihood of bond failure.

### Results:

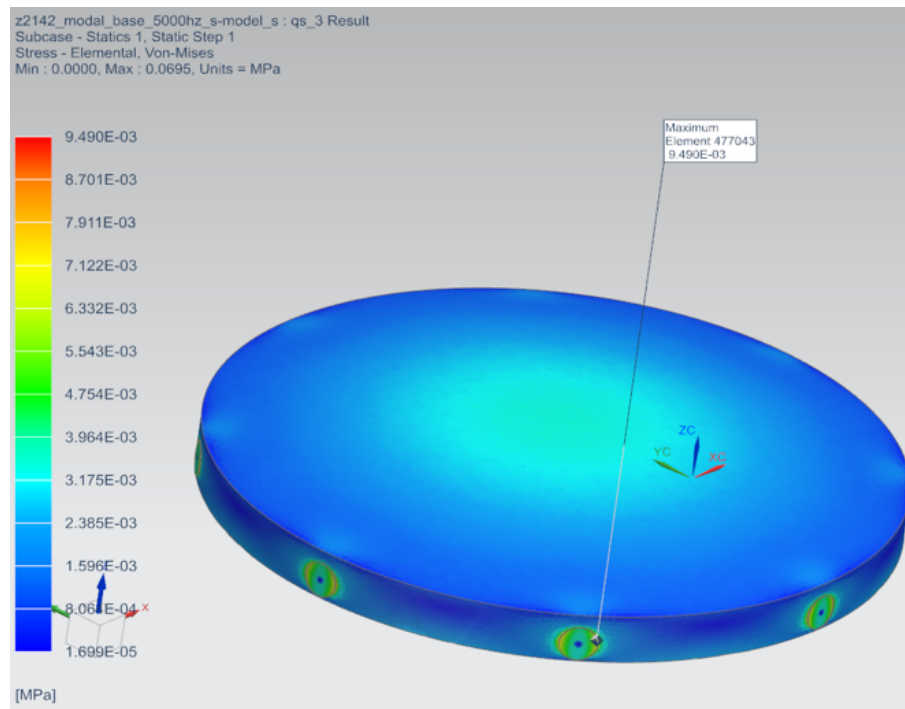


Figure 3.15: Glue spots analysis on a constrained lens

The test data demonstrate that the current design employs lens curvature and a strategic arrangement of adhesive spots, exhibiting superior resistance to applied forces. Conservative calculations based on test-derived allowables estimated a maximum load of approximately 3000 N. However, experimental results demonstrated that the assembly could withstand compressive forces up to 4500 N. This discrepancy suggests that the design's geometry effectively transfers the load through combined shear and compression, enabling the adhesive joint to sustain significantly higher stresses than initially predicted.

## 3.2. EP42HT-2LTE

The structural adhesive EP42HT-2LTE was tested to evaluate its properties in bonding configurations between invar and fused silica and between fused silica and fused silica. This adhesive, described as high performance in the datasheet [15], has a stated tensile strength of 41 MPa for aluminum/aluminum bonding. Characterized by an exceptionally low coefficient of thermal expansion and low linear and volumetric shrinkage, it is designed for critical applications, such as those in aerospace, optics, and cryogenics. Therefore, the low coefficient of thermal expansion makes it particularly efficient for glass-to-glass bonding, considering that among the various available adhesives, it has the lowest CTE, it would introduce less residual stress in glass that has CTE close to zero.

### 3.2.1. Tensile test

For the fused silica/fused silica configuration, specific arrangements were made to avoid damage to the substrate of the specimen and ensure a stable connection to the test machine. Steel supports were used to connect the specimens to the machine, avoiding applying stresses directly on the brittle glass.

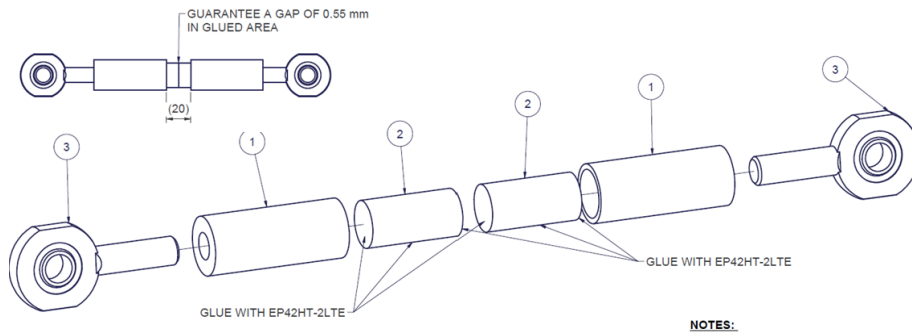


Figure 3.16: Tensile test specimen

Tensile test results showed consistent behavior, with a strength limit of about 20 MPa for the fused silica/fused silica system. Although lower than the datasheet value (41 MPa for aluminum/aluminum), this result is consistent with substrate differences and expectations for bonding based on brittle materials such as fused silica. The dispersion of the results was limited, confirming the reliability of the adhesive under these conditions with a standard deviation of 1.65 MPa (Figure 3.17).

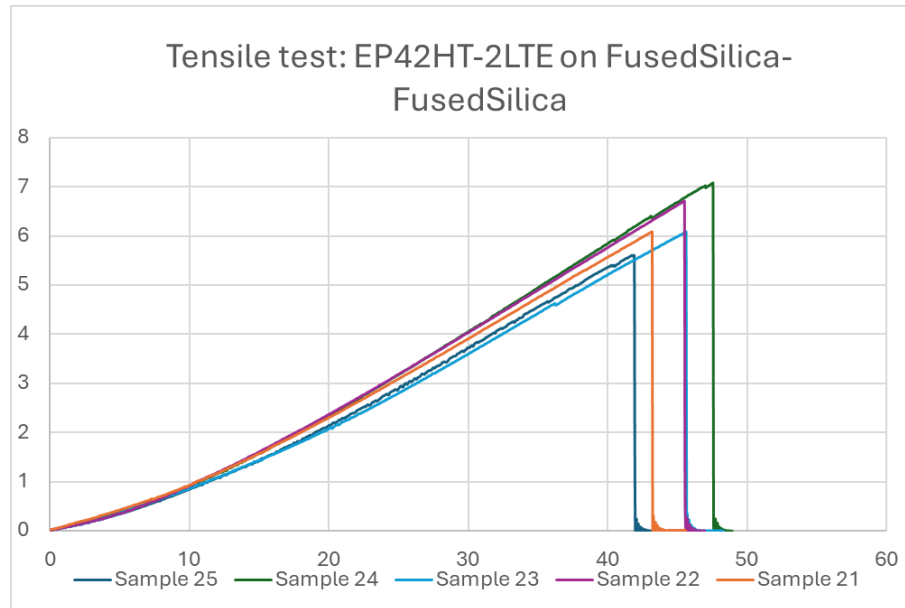


Figure 3.17: Tensile test results

### 3.2.2. Shear test

Shear test specimens were designed with a geometry intended to minimize bending contributions. Despite these design efforts, bending moments could not be completely eliminated and, in several specimens, led to premature failure of the glass substrate. This premature failure compromised the collection of complete adhesive data. The inherent geometric complexity of the specimens, combined with the brittleness of fused silica, further complicated the analysis. In some cases, the glass substrate broke before the adhesive reached its failure limit, making it difficult to determine a definitive strength value for the adhesive.

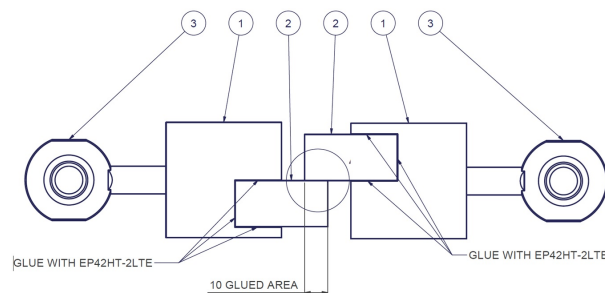


Figure 3.18: Shear specimen

However, when the stress in the adhesive was analyzed at the point of specimen failure, the following key observations were made:

- The minimum adhesive strength recorded exceeded 9.5 MPa.
- The dispersion of the results was acceptable, with a variation of approximately 15.3 percent and a standard deviation of 1.5 MPa.

Although the measured shear strength is somewhat lower than the datasheet values, it is still adequate for non-critical applications.

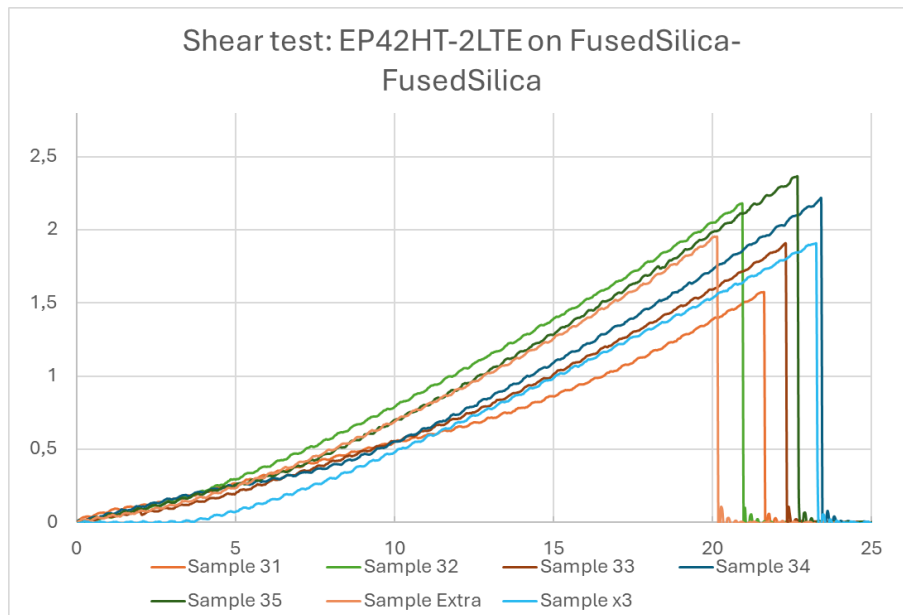


Figure 3.19: Shear test results

In the context of shear tests, the collection of data was found to be partially compromised by the occurrence of premature substrate failure. The results that were obtained, however, do provide indications of an adhesive strength that is considered to be within an acceptable range. The unique properties of EP42HT-2LTE, such as its low coefficient of thermal expansion and its excellent dimensional stability, render it particularly well-suited for advanced technical settings, particularly in the domains of optical or cryogenic applications. It is imperative to acknowledge that the behavior of adhesives exhibits significant variations depending on the substrate utilized. Consequently, test results for glass or germanium substrates may not be directly comparable to datasheet values derived from aluminum-to-aluminum bonding.

### 3.3. Manufacturing and integration phase

Following a preliminary examination of the structural adhesives and a determination that they are suited to the application, the subsequent step is to analyze their behavior in the context of a project involving more complex geometries.

In addition to the structural checks required to ensure the strength of a component during its operational life, when dealing with delicate objects, such as those used in the optical industry, it is essential to ensure that they are not damaged during assembly and integration. In this regard, two particularly critical processes have been identified in the component integration phase: the installation of optical fibers and the curing process of epoxy and silicone glues applied to a lens or other critical points of a component.

In the following example, we will examine a complex component from a telescope that contains various types of adhesives. These adhesives include two structural adhesives previously discussed (EP42HT-2LTE and EC2216), as well as a silicone adhesive utilized as a sealant and to absorb shocks (MS323AO-LO). The primary objective of this subsequent analysis is to ascertain whether the diverse materials exhibit stress due to disparate CTE during a thermal load or due to the shrinkage of the adhesive during its cure phase.

#### 3.3.1. Stress induced by the shrinkage of the adhesive

For the component under consideration, a shrinkage analysis of the EP42HT-LTE adhesive is required. Although this adhesive exhibits very little volumetric change and is certified for applications of this type, it is still good practice to verify the stress induced by volumetric shrinkage on the fibers. The contact of this adhesive with crucial components such as optical fiber imposes an analysis of this type.

A non-linear analysis is employed to simulate the shrinkage of the adhesive by leveraging its pre-existing model properties, such as the CTE. In this case, as in others where shrinkage is present, finite element analysis (FEM) can be conducted using the thermoelastic analysis function commonly found in major FEM software. All materials, except those subject to shrinkage, are considered to have a coefficient of thermal expansion (CTE) of zero. Adhesive shrinkage, equal to a volumetric change of 0.01%, is simulated by finding the temperature change  $\Delta T$  corresponding to a volume reduction equivalent to that occurring during the curing phase. In this case:

$$\frac{\Delta l}{l_0} = CTE * \Delta T = 0.0001 \rightarrow \Delta T = \frac{0.0001}{12e^{-6}} = 83.3C$$

Such an analysis is rather conservative since the modulus of elasticity of the adhesive considered does not correspond to the actual value [26] [29]. In fact, during the curing phase, the adhesive's modulus of elasticity gradually increases until it reaches its final value, as indicated in the datasheet and confirmed by the tests performed. The modulus of elasticity ( $E$ ) presents a linear variation with temperature and reaches its maximum value at the completion of the shrinkage process. A conservative approach is taken by setting the initial value of  $E$  at 5MPa, thus preventing it from starting at 0.

The non-linear analysis reveals that the shrinkage gives rise to a stress of approximately 0.43 MPa in the adhesive, which is well below the acceptable limit for the fiber optic stress limit. An alternative analysis was also carried out, taking into account the stiffness of the adhesive at its maximum level during the entire shrinkage phase, which gives a stress of  $\sim 5MPa$  in the optical fibre, still below the limit but without a good margin (3.20 (a)). However, even though the Young's modulus state during curing is unknown, it's reasonable to approximate it with a linear behaviour.

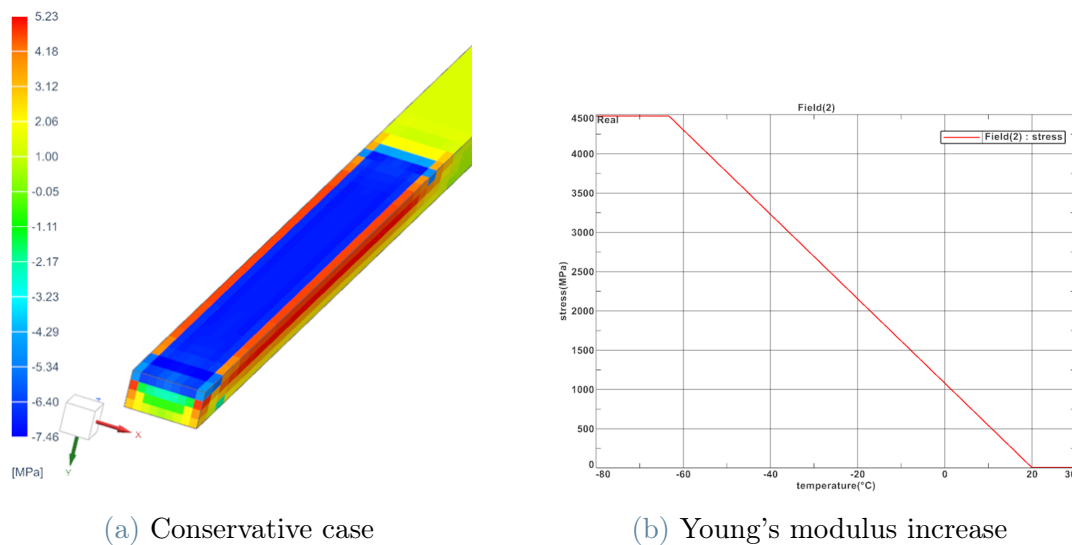


Figure 3.20: Shrinkage simulation

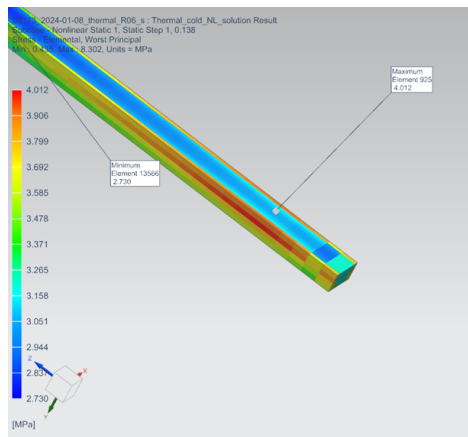
### 3.3.2. Stress induced by the difference in CTE

A similar analysis was conducted for both the EP42HT-LTE and EC2216 adhesive, which are placed in a critical location where they may induce stress on the optical fiber, the most sensitive component of the structure.

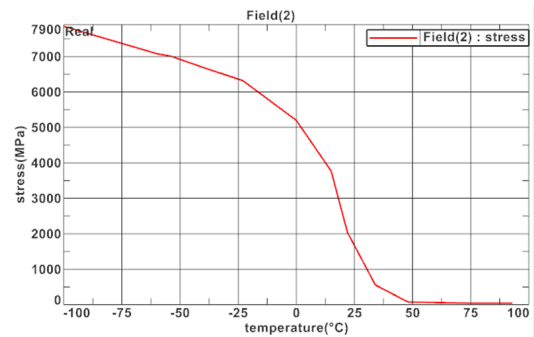
Two simulations were performed to approximate the thermal effects on the adhesive. In the first simulation, the adhesive's coefficient of thermal expansion (CTE) was modeled

as a function of temperature, capturing its variation across different thermal conditions. In a more conservative second simulation, the maximum CTE value was used to represent worst-case conditions. The stress analysis of both the adhesive and the optical fiber revealed that high stress levels primarily result from the adhesive’s CTE combined with an increased tensile modulus in cold conditions.

The worst-case scenario reported a stress in the optical fiber of 10.7 MPa, while in the more realistic scenario where the CTE varies with temperature is 4 MPa.

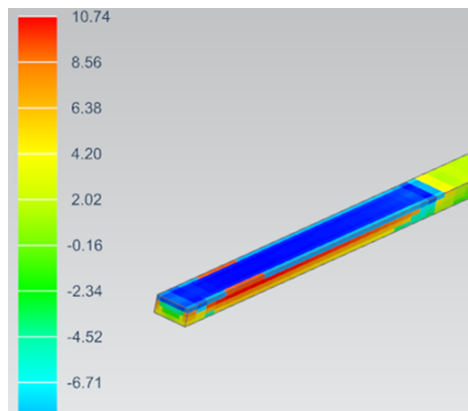


(a) Stress in optical fiber

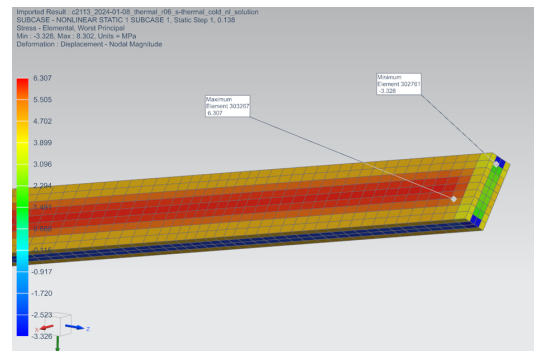


(b) CTE trend with temperature

Figure 3.21: Thermoelastic analysis with CTE defined with temperature



(a) Stress in the optical fiber



(b) Stress in the EC2216 adhesive

Figure 3.22: Thermoelastic analysis with fixed CTE

It is important to note that this elevated stress is typically not observed when the two materials bonded together have similar CTE values (as discussed by Côté and Desnoyers in [6])

The formula from Yoder is used to assess the thermoelastic stress in the EC2216. The stress is very low, it is not considered an issue.

The stress in the EP42HT-2LTE is near zero; the two joined parts have the same CTE

$$\tau_{\max} = \frac{(CTE_1 - CTE_2)\Delta TG \tanh(\beta l)}{\beta t}$$

$$\beta = \left[ \frac{G}{t} \left( \frac{1}{E_1 h_1} + \frac{1}{E_2 h_2} \right) \right]^{\frac{1}{2}}$$

that gives a  $\tau_{max}$  of 8.16 MPa.

### 3.3.3. Integration of the optical fibers

**Stress induced by the curvature of the axis of the OF:** In our design, the optical fiber is firmly bonded along a flat Invar 32-5 surface so that bending is completely prevented along most of its length. However, a small section near the fiber's termination is left unconstrained (with a gap of a few millimeters) to allow for slight bending when the fiber is inserted into a housing. The key challenge is to determine the optimal length of this free segment so that the fiber can flex without incurring damage.

A comprehensive analysis was carried out using both 3D and 2D finite element models to evaluate the bending behavior of the optical fiber under a small displacement of 0.1 mm, which is considered to be the minimum displacement that can be guaranteed during manufacturing. The objective was to determine the necessary inflection length required to keep the maximum stress on the fiber below its critical 25 MPa rupture limit.

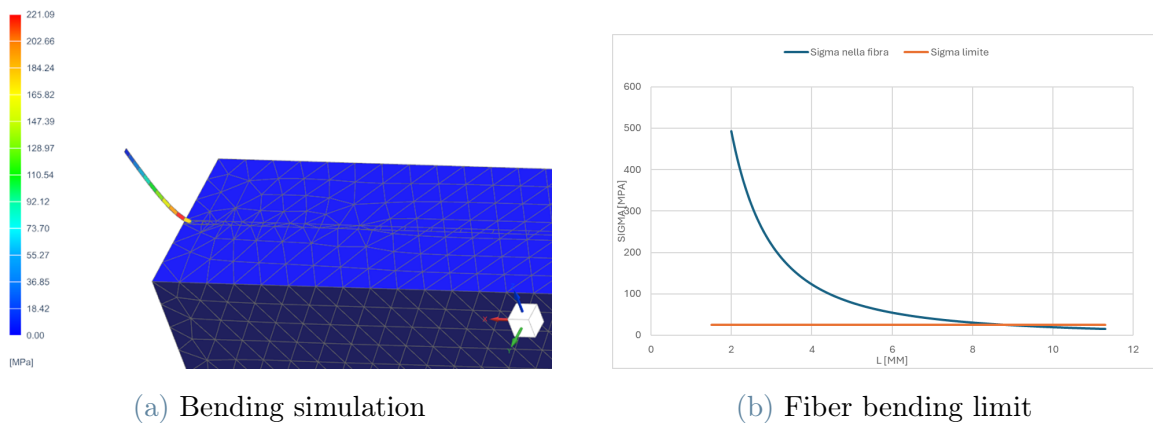


Figure 3.23: Stress in the optical fiber vs. Maximum stress allowable in the fiber

#### Results and Design Implications:

The analysis revealed that an inflection length of 2 mm (or 3.5 mm when including the portion of the fiber that remains in contact with the plate but is not bonded) is insufficient to ensure that the maximum stress does not exceed the 25 MPa threshold. Simulation results indicate that a free fiber length of approximately 8.5 mm is required to maintain stress levels below this critical limit. This finding necessitated a design revision to develop an integration procedure that prevents fiber damage.

Three potential solutions were proposed:

1. Cut a section of the Invar plate beneath the fibers to create the necessary space for fiber bending.
2. Apply the adhesive after the fiber has been aligned with the second component.

3. Position the adhesive layer further away from the fiber so that the fiber end remains free to move.

The second solution was rejected because the high viscosity of the adhesive tends to misalign the fibers.

### Analysis and Design Considerations:

Initially, the integration procedure maintained the second metal support in a fixed, perpendicular orientation relative to the fiber. This configuration effectively locked the fiber at the end, resulting in excessive bending stress that would require an impractically long unconstrained segment to prevent breakage. Consequently, this approach was discarded in favor of a design that permits the second support to rotate freely. Allowing rotation reduces the bending strain on the fiber, thereby enabling a shorter, more practical length of unconstrained fiber while still ensuring reliable performance.

To give the fiber a chance to deform further, the optical fiber has been decided to leave it unconstrained on the plate as seen in figure 3.24. It is first glued at one tip and then at the other, with the second tip fixed against a reference plate. This procedure introduces stress into the fiber. Assuming the fiber behaves like a cantilever beam, its stress can be approximated as a function of the deflection ( $d$ ) by the following relationship:

$$\sigma = \frac{3 \cdot E \cdot d \cdot h/2}{l^2}$$

where the modulus of elasticity of the fiber is  $E = 73GPa$ , the height of the fiber is  $h = 0.18mm$ , and  $l$  the free length of the fiber of 57.6 mm. The stress calculated with a displacement of 0.1 mm is 0.6 Mpa, which is an admissible result.

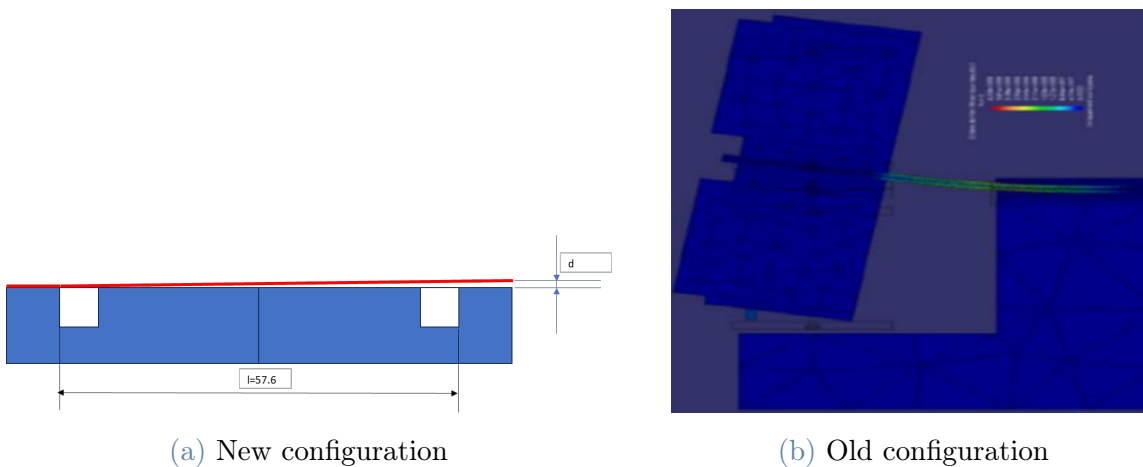


Figure 3.24: Optical fiber bending at the tip

### 3.4. Considerations on Two-Component Epoxy Adhesives

The epoxy adhesives EP42HT-2LTE and EC2216 have been considered for structural bonding projects, both proving adequate for their intended purpose. However, some differences in their physical properties and operational characteristics make the choice between the two dependent on a number of project-specific factors. Below, the main aspects of differentiation are analyzed.

#### **Stiffness and Thermal Adaptability:**

EP42HT-2LTE adhesive, due to its high stiffness modulus and ability to provide high mechanical strength, is ideal for applications that require a small contact surface area. However, in applications involving materials with different coefficients of thermal expansion (CTEs), such as lenses and substrates with different CTEs, its stiffness may introduce higher stresses. This is critical in cases where the lens is over-stressed, increasing the risk of stress induced in the substrate and compromising structural integrity.

EC2216 adhesive is more tolerant to thermal and mechanical stresses caused by differences in CTEs due to its higher elastic deformation capacity. In projects requiring greater flexibility or more accurate stress control, EC2216 may be a preferable choice.

#### **Pot-Life and Applicability:**

The pot life of EP42HT-2LTE adhesive, while sufficient for standard applications, is shorter than that of EC2216. In addition, the preparation process requires careful mixing and the use of an agitator to maximize the pot life for application. This can complicate use in configurations involving precise and slow applications, such as those made with syringes or in small channels.

EC2216 adhesive is more convenient to use due to a longer pot life, 20-25 minutes longer than EP42HT-2LTE. In addition, as it was already widely used in the company, its application process was optimized for existing operational needs.

#### **Cost and Procurement:**

EC2216 is advantageous for small-scale applications due to the availability of small package sizes, which reduce the risk of waste, considering the shelf life of the adhesive once opened.

Although the cost per batch may be higher, Master Bond's EP42HT-2LTE stands out for customer support, offering customized solutions for specific needs, such as providing

appropriate packaging for custom or small-batch projects.

### **Conclusions**

The choice between EP42HT-2LTE and EC2216 strongly depends on the needs of the project:

EP42HT-2LTE is ideal for high mechanical strength applications where high stiffness and dimensional accuracy are required, especially in critical environments such as aerospace or optics. However, its use must be carefully evaluated in the presence of materials with divergent CTEs to avoid undesirable stresses.

On the other hand, EC2216 is preferred in designs that require greater operational flexibility, more tolerant behavior to thermal and mechanical stresses, and simplified handling due to its higher pot-life and lower risk of waste.

Economic and technical evaluation must therefore be conducted on a case-by-case basis, considering both project requirements and operational and logistical constraints.

# 4 | Non structural adhesives

## 4.1. Nusil CV1142

In addition to adhesives with a purely structural function, silicone adhesives, such as Nusil CV1142, used mainly along the edge of the lens, were also considered in the telescope design under consideration. This adhesive is not designed to withstand high tensile loads, but its pliability makes it ideal for absorbing any deformation of the lens, fixing it, and dampening vibrations without introducing additional stresses, unlike the structural adhesives used for the main attachment points. Nusil CV1142 has a number of advantages that make it particularly suitable for space applications:

- High temperature resistance, ensuring its stability in extreme environments.
- Single-component composition, which simplifies its application.
- High viscosity, which prevents dripping, making it usable even on vertical surfaces.

The ductility of this adhesive allows it to function as a filler material, reducing the effects of shock and vibration. However, its tensile limit, stated as 4.1 MPa in the datasheet, makes it unsuitable for resisting significant loads. For this reason, failure of the adhesive is considered at first release during the simulation phase, since the actual behavior is less predictable than with structural adhesives.

### Tests and simulations

In the simulation phase, the Nusil CV1142 adhesive is modeled with conservative parameters to identify any unexpected critical points. The simulations were supplemented with experimental tests, aimed at validating both the properties of the adhesive and the application of a primer on the adhered surfaces.

One of the problems that emerged during the tests is the tendency of the adhesive to fail by complete adhesive detachment, pulling away entirely from one of the bonding surfaces. Although the application of a primer was shown to significantly improve this behavior by increasing the strength limit of the adhesive, it was unable to eliminate it completely.

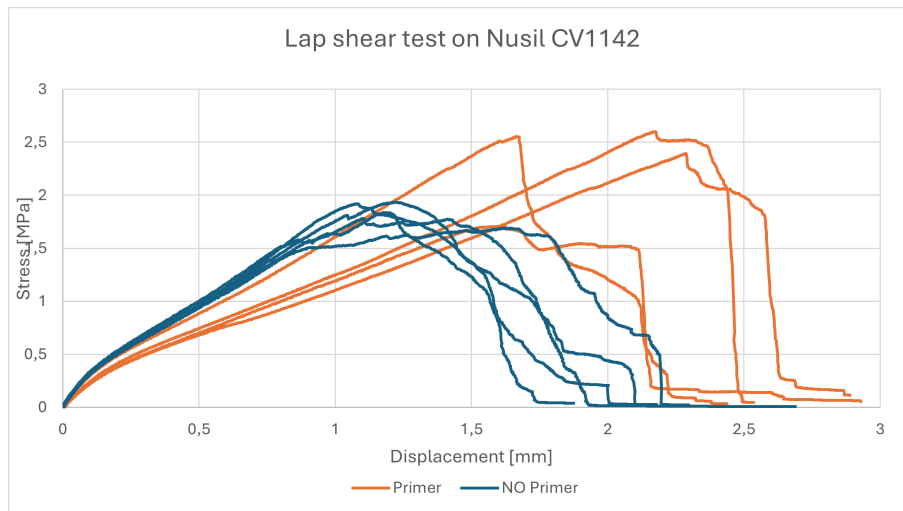


Figure 4.1: Shear test results

From the results of the tests conducted, it is shown that the application of a primer significantly improves the maximum strength of the adhesive joint. However, this treatment introduces more variability in the behavior of the adhesive, making it less predictable than in tests without primer.

**With Primer:** Higher maximum strength of the joint, but the observed failure tends to be a combination of cohesive failure (failure within the adhesive material) and adhesive failure (detachment from the adhesive interface). This combination introduces more scatter in the results, complicating the predictivity of joint behavior. The mean adhesive strength is 2.3 MPa and the standard deviation is 0.35 MPa.

**Without Primer:** The joint exhibits purely adhesive failure, characterized by more uniform and consistent strength values. This behavior makes the adhesive more predictable, but with a lower strength than primer-treated specimens. The mean adhesive strength is 1.78 MPa and the standard deviation is 0.15 MPa.

### Application implications

Primer application can be advantageous in cases where the strength of the adhesive joint needs to be maximized. However, it is critical to consider that less predictable behavior could be a critical issue in applications where high repeatability of performance is required.

One possible solution is further optimization of primer and adhesive application conditions to reduce variability in results, thereby improving overall joint reliability.

### Simulation

The high viscosity and consistency of the adhesive resulted in specimens with imperfect

corners and minor adhesive overflow. This provided an opportunity to test the findings of Zhao et al.[27] regarding single lap joint simulations with rounded corners.

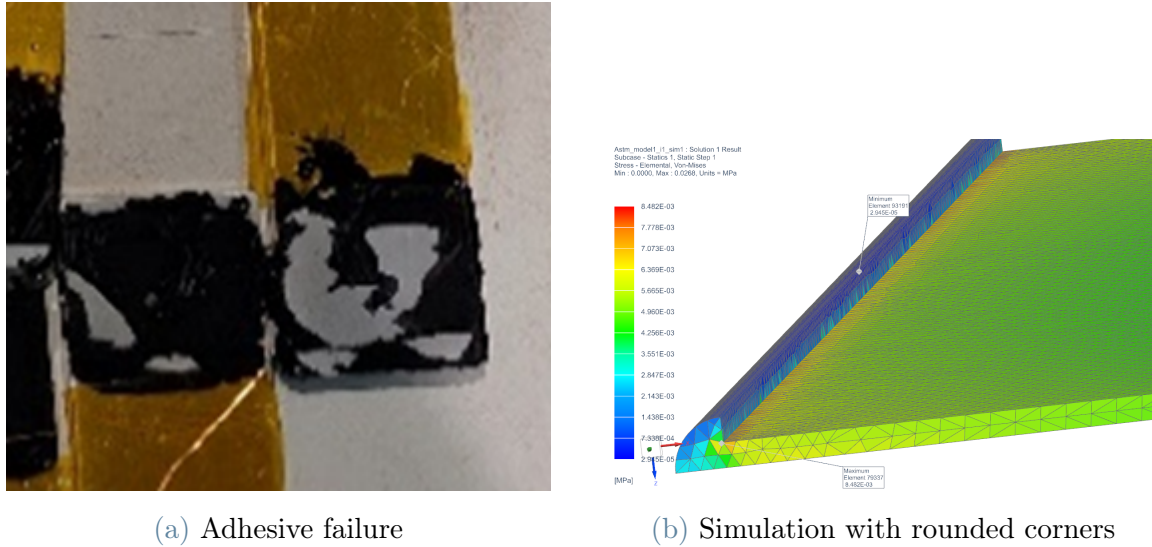


Figure 4.2: Adhesive layer model

Simulating single lap joints with rounded adherend corners provides a more realistic representation of the actual manufacturing conditions by eliminating the stress singularities associated with sharp corners. Sharp corners produce mathematical singularities (infinite stresses) that complicate analysis, by rounding the corners, the stress and strain fields become finite and more manageable. This approach results in finite stress and strain fields, thereby enabling more reliable finite element analyses and improved strength predictions. In brittle adhesives, an increase in joint strength of up to 40% was observed with a larger radius. However, the simulation's accuracy can be affected by mesh sensitivity near stress concentrations, as well as by the inherent difficulties in capturing the effects of pre-existing defects.

## 4.2. Thermoelastic analysis: C2302 EAGLET

An application case of thermoelastic analysis involves the telescope model called EAGLET. The assembly consists of a set of lenses fixed on a titanium alloy substrate and stabilized by adhesive. Among the different lenses of the telescope, the most critical lens was identified, on which a thermal analysis was conducted to assess the criticality arising from the joint and the influence of the stresses on the overall deformation of the lens (Figure 4.4).

The objective of the present analysis is to identify any deformation of the lens surface in

order to extract Zernike's coefficients and to inspect potential aberrations in the optical field, as discussed in Chapter 2.

Two adhesive were selected for this application: the Nusil CV1142-2 and the MasterSil 323AO-LO. The adhesive properties of the previously analyzed Nusil CV1142 are compared with those of a stiffer competitor's product. The role of the adhesive is not structural; therefore, the objective of the analysis is to determine the most suitable option for utilization.

|                              | <b>CV1142-2</b>           | <b>MasterSil</b>                                       | <b>Comments</b>   |
|------------------------------|---------------------------|--|---|
| <b>E [Mpa]</b>               | 2MPa<br>(rough estimate)  | 3.4 – 4.8 MPa  |   |
| <b>CTE [ppm/°C]</b>          | 320                       | 140-170<br>(average 155)                               | Lower CTE is better (less in-plane deformation of the mirror) |
| <b>Viscosity [cps]</b>       | N/A                       | 300,000 – 400,000                                      |   |
| <b>Shrinkage</b>             | N/A                       | Low shrinkage<br>(no solvent)                          |   |
| <b>Working life</b>          | 15 min (tack-free time)   | 2-3 hours  | More time to align  |
| <b>Mono/<br/>Bicomponent</b> | Monocomponent             | Bicomponent  | Bi-component = cure guaranteed                                |
| <b>Cure cycle</b>            | 7 days @ room temperature | 3 days or 2 days at room temperature + 3 hours at 50°C |   |

Table 4.1: Silicone adhesive comparison

One of the main temperature-related problems is the strain induced by the difference in the thermal expansion coefficients between the lens and the barrel. The lens, made of Fused silica glass, has a coefficient of thermal expansion (CTE) close to zero ( $0.52 \times 10^{-6}$ ), while the CTE of the titanium barrel and adhesive is significantly higher.

A critical issue is the geometry of the bonding area. In the region where the lens directly contacts the titanium substrate, high stresses are generated even with small temperature gradients. This problem is caused by interference between the barrel edge and the lens, which produces inaccurate analysis due to excessively high strains. Two models were created to simulate the adhesive layer:

1. Model 1: simple geometry without adhesive slipping between the glass and metal
2. Model 2: with a small space to insert the adhesive between the lens and the barrel.

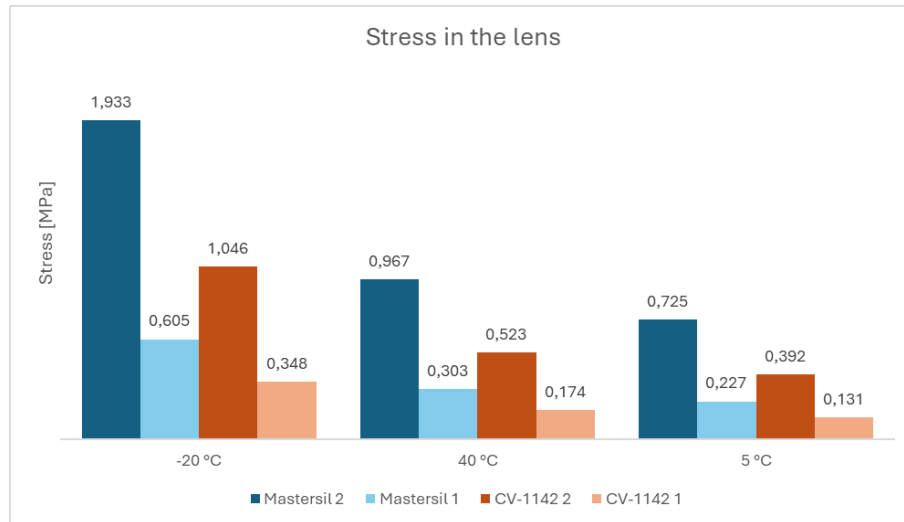


Figure 4.3: Stress induced in the lens by the adhesive comparison in different scenarios

Contrary to expectations, the analysis shows that CV-1142 glue performs better than Mastersil because of its lower stiffness ( $E$ ), which mitigates the effects of the high coefficient of thermal expansion ( $CTE$ ).

In Model 2, the inclusion of additional adhesive between glass and metal led to worse results, as the addition of a material with high  $CTE$  increased the stresses due to thermal variations. This is because, the additional adhesive layer is modeled with a greater thickness than in reality to simplify modeling and according to the size of the elements.

The scope of the analysis is to

### Finite element model convergence

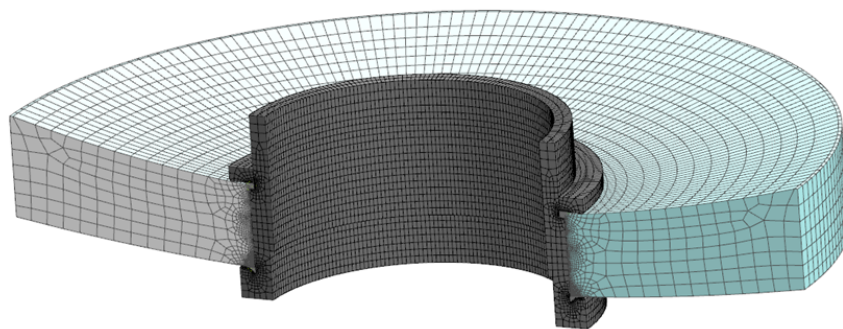


Figure 4.4: Finite element model of the lens fixed to the barrel

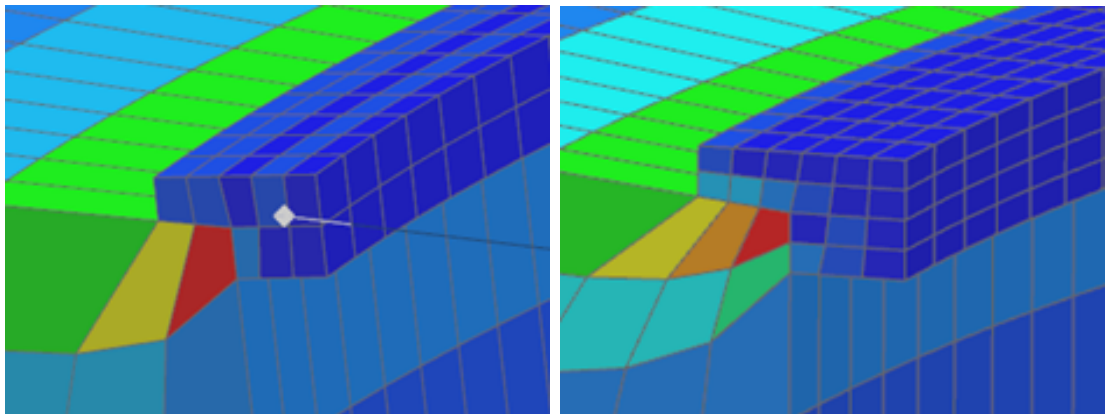
The model was developed using a structured mesh. Due to symmetry with respect to the central axis of the object, the mesh of a single section was made, then extruded by revolution around the axis. Compared with a tetrahedral mesh, the structured mesh offers several advantages:

- Greater precision in stress distribution: The uniformity of the structured mesh enables accurate stress analysis, improving the representation of actual physical behavior and the reliability of results.
- Improved computational efficiency: The organized arrangement of structured meshes reduces computational load, simplifying numerical operations and accelerating convergence. This is critical in large-scale or high-fidelity simulations where computational resources are a constraint.
- Stability and convergence: The regularity of elements and predictable grid ensure uniform mapping of variables between nodes, contributing to algorithmic stability and consistent convergence in FEA analysis.

A convergence study was conducted on the model's glue layer, using mesh sections with variations in the number of elements along the thickness (Figure 4.5). The structured mesh, selected for its regularity, offers stability and consistency in the results as the number of elements varies, mainly due to the rotational geometry of the model, which allows the extrusion of a 2D grid of elements around the central axis.

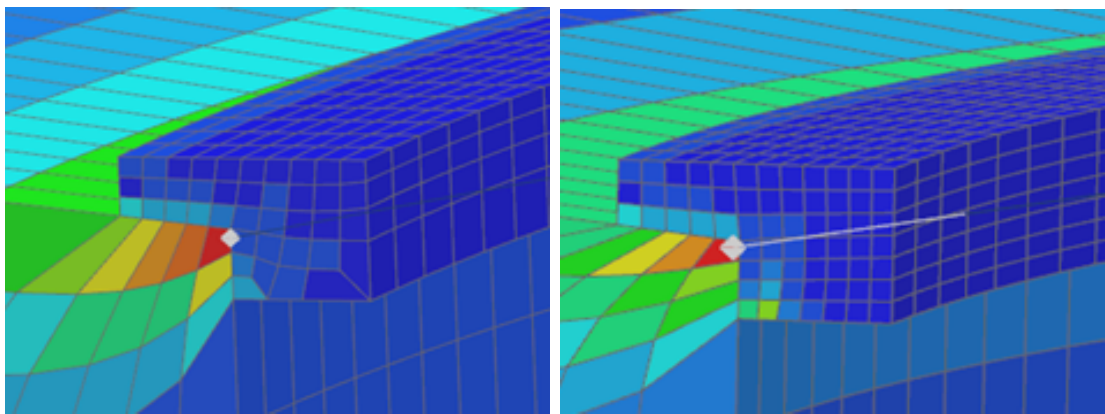
In FEA, convergence represents the process of bringing the simulated solution closer to the exact solution of partial differential equations (PDEs) through progressive mesh refinement. In structured meshes, the reduction of the element size improves accuracy by sampling the physical domain in greater detail. The expected convergence for a 3D structured mesh depends on both the size of the elements and the overall quality of the mesh.

In this case, acceptable results were achieved with a mesh of only three elements in thickness, avoiding the high computational cost of a more detailed mesh, disproportionate to the needs of the analysis. It should be remembered that the main objective is to understand the deformation of the lens surface, which can be compensated for by modifications to the optical design management software.



(a) 1 element

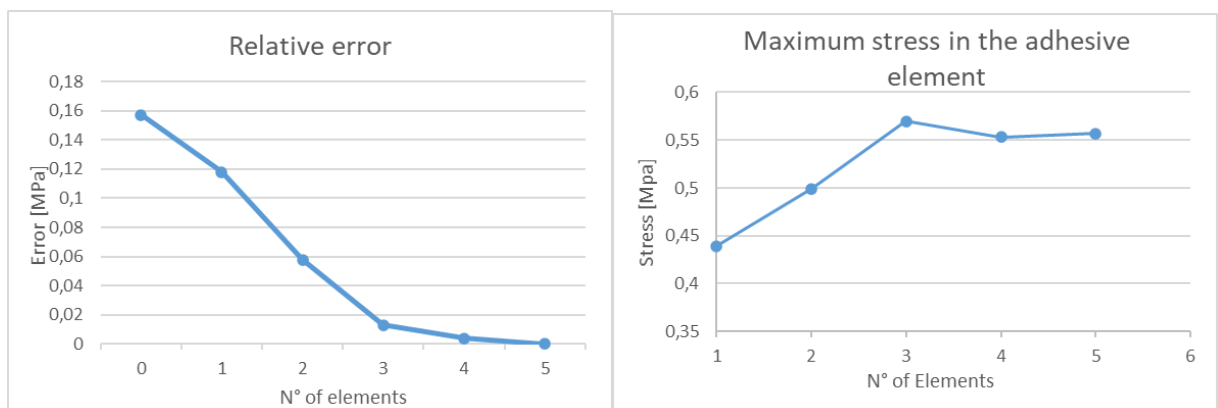
(b) 2 elements



(c) 3 elements

(d) 4 elements

Figure 4.5: Elements in the structured mesh



(a)

(b)

Figure 4.6: Convergence

### 4.3. RTV566

An in-depth analysis and testing program was conducted on RTV566 adhesive: a two-component silicone formulated for low outgassing applications and used primarily as an electrical insulator. Specimens featuring SuperInvar and Fused Silica (glass) surfaces were employed to assess both tensile and shear performance. Although RTV566 is noted for its high chemical stability and excellent insulating capacity, its structural properties are limited.

#### Specimen Geometry and Test Configuration:

Due to the brittle nature of fused silica, special arrangements were necessary for specimen preparation:

- **Tensile Testing:** To avoid directly bonding the fused silica to the tensile machine (which would induce unwanted stresses), superinvar intermediate supports were used. These supports were bonded to both faces of the specimen, minimizing extraneous stress during testing.

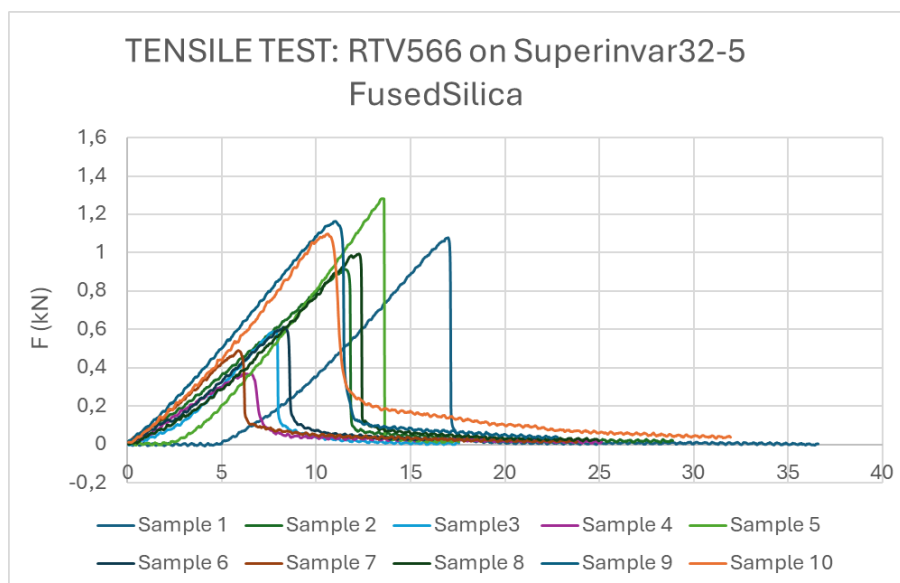


Figure 4.7: Tensile test results

- **Shear Testing:** Specimens were designed with specific geometries to reduce bending moments. Despite these efforts, the inherent complexity of the joint and the adhesive's low structural performance complicated result interpretation.

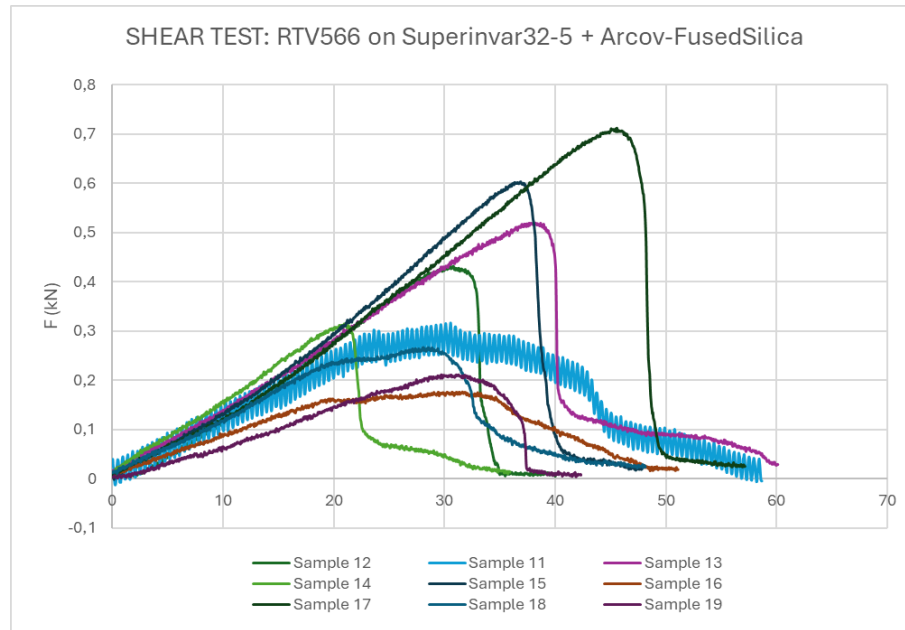


Figure 4.8: Shear test results

### Test Results and Analysis:

The experimental results indicated that the RTV566 adhesive did not cause failure in either the fused silica or the superinvar substrates; failure was confined solely to the adhesive layer. However, several key observations emerged:

1. **Result Dispersion:** The strength values recorded in both tensile and shear tests exhibited variability exceeding the acceptable 20 percent threshold. This high dispersion makes the adhesive's performance less predictable and complicates the quantitative assessment of its true strength.
2. **Unpredictable Behavior:** Consistent with other nonstructural adhesives, the point of release does not always correlate with the nominal strength limit. This discrepancy is likely due to the adhesive's limited ability to transmit loads and its formulation for specific, low-stress applications.
3. **Structural Limitations:** The tests confirmed that RTV566 is unsuitable for structural applications, as the adhesive failed at loads significantly below those achieved with previous adhesive formulations. Even with proper primer application and controlled processing, the bond failure was attributed to the inherent limitations of the adhesive's structural performance.

### Conclusion:

RTV566 adhesive demonstrates adequate performance for electrical insulation and similar



Figure 4.9: Adhesive failure in RTV566

nonstructural applications owing to its chemical stability and insulating properties. However, the significant dispersion in test results, unpredictable failure behavior, and early adhesive failure confirm that it is not appropriate for structural bonding where higher load-bearing capacity is required.

#### 4.4. NOA 88

Norland Optical Adhesive 88 (NOA 88) is a UV-curable adhesive renowned for its excellent optical clarity, low shrinkage, and high bond strength. It's used in most optical assemblies inside the company. NOA 88 is particularly valuable in applications requiring precise alignment and stable bonding of components such as lenses, filters, and optical fibers. Moreover, it satisfies the prerequisite for space applications and is heavily used in projects by both ESA and NASA. This chapter reviews the key properties of NOA 88, its performance in optical applications, and its suitability for space projects, drawing on both direct experimental experience and published technical data.

NOA 88 exhibits good bond strength and durability, with a rapid UV-curing process that ensures minimal shrinkage and high dimensional stability. It offers optical clarity across the visible and near-infrared spectrum, making it ideal for bonding optical components. In our direct experience assembling precision optical instruments, NOA 88 provided consis-

tent and robust adhesion between glass lenses and other substrates. The adhesive's high shear strength, as indicated in its datasheet (Norland Optical Adhesive 88 Datasheet, Norland Products, 2021), enables it to maintain strong bonds even under significant mechanical loads. This performance is critical in optical systems, where any misalignment or distortion can lead to aberrations and degraded image quality. We tested this adhesive both in shear and tensile strength on Titanium and Glass substrates.

### Tensile test

For this test, the same specimen is used for all the other tensile tests. The results obtained are lower than the expected datasheet values, with a minimum of 2.7 MPa and an average of 6.6 MPa. However, there is considerable variation in the test results, which can only be attributed to the superficial conditions of the titanium substrate, with a standard variation of 3.4 MPa.

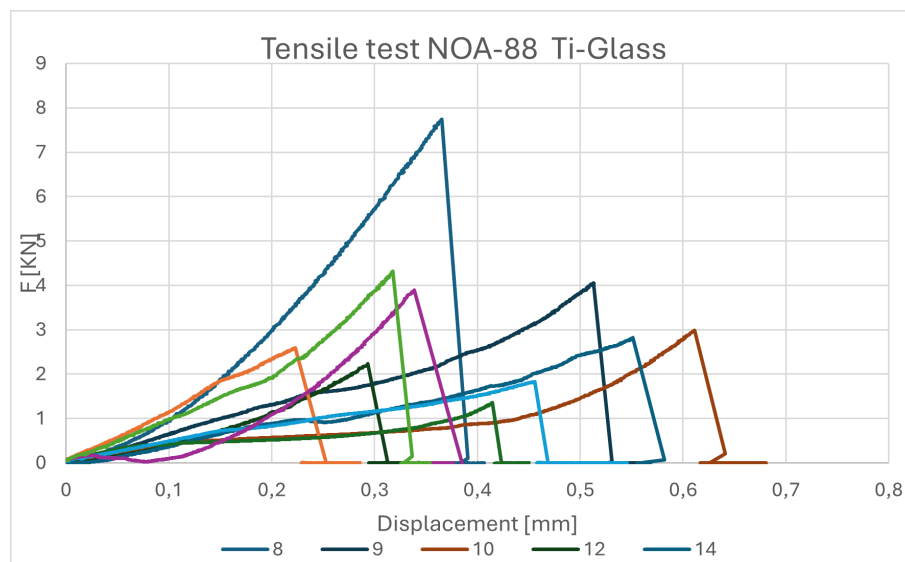


Figure 4.10: Tensile test results

### Shear test

In this case, the same specimen used in the EC2216 shear test with SuperInvar and fused silica is employed. The expected shear strength is lower than the value stated in the datasheet, due to the effects of bending and shear stresses, although it remains within an acceptable range. The minimum stress is 6 MPa, the average 7.7 MPa with a standard deviation of 1.6 MPa.

The adhesive's low thickness is advantageous in shear conditions, as it impedes peel occurrence and reduces the adhesive layer's compliance, thereby enhancing its performance under shear. Furthermore, the experimental findings indicate that surface treatment

enhances the adhesive's performance, specifically the surface's smoothing. This is particularly relevant in scenarios where the adhesive is employed to connect two optical components, which often possess smoother surfaces compared to metal.

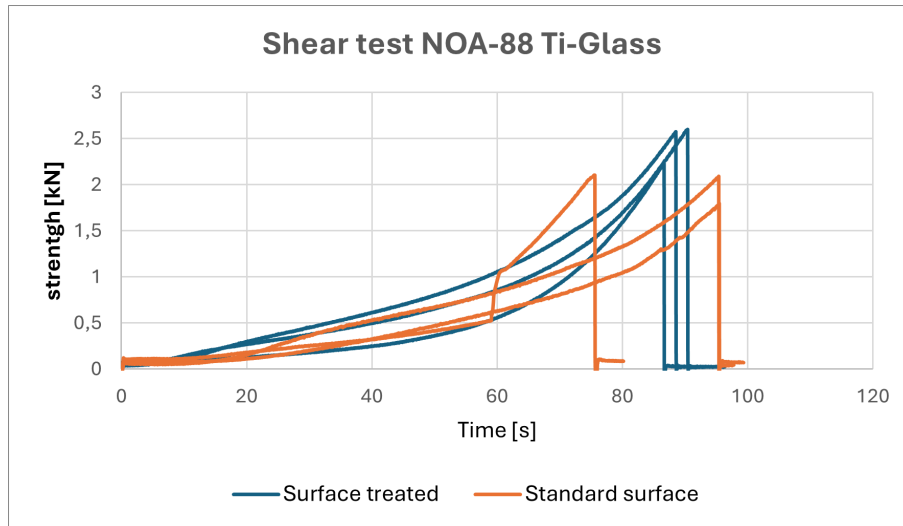


Figure 4.11: Shear test results comparison

## Simulations

In order to simulate the NOA 88 adhesive in Simcenter 3D, penalty contact has been used. The formulation of penalty contact in finite element analysis (FEA) offers an efficient method for simulating thin adhesive layers. This is achieved by applying a virtual stiffness based on the adhesive's properties, including its modulus, thickness, and Poisson's ratio. This approach eliminates the necessity for explicit meshing of the adhesive layer, thereby allowing the use of less refined meshes and a reduction in computational cost. Penalty contact formulations work by introducing a virtual stiffness (penalty parameter) that penalizes any penetration between contacting surfaces, enforcing contact without requiring an exact kinematic constraint. When simulating an adhesive bond, the penalty parameter can be tuned to mimic the adhesive's elastic response, effectively replicating the behavior of a very thin adhesive layer.

To successfully implement a penalty contact formulation, it is essential to know the adhesive's material properties, such as:

1. Elastic Modulus of the adhesive ( $E_{Adhesive}$ )
2. Elastic Modulus of the substrate ( $E_{Source}$ )
3. Thickness of the adhesive layer
4. Poisson's Ratio: Helps define the overall deformation characteristics under load.

$$PENN = \frac{E_{Adhesive}}{E_{Source} * t_{Adhesive}}$$

In our Simcenter 3D simulations of NOA 88, this approach allowed us to replicate experimental shear and tensile behaviors without requiring an overly refined mesh, thus reducing computational cost while maintaining accuracy.

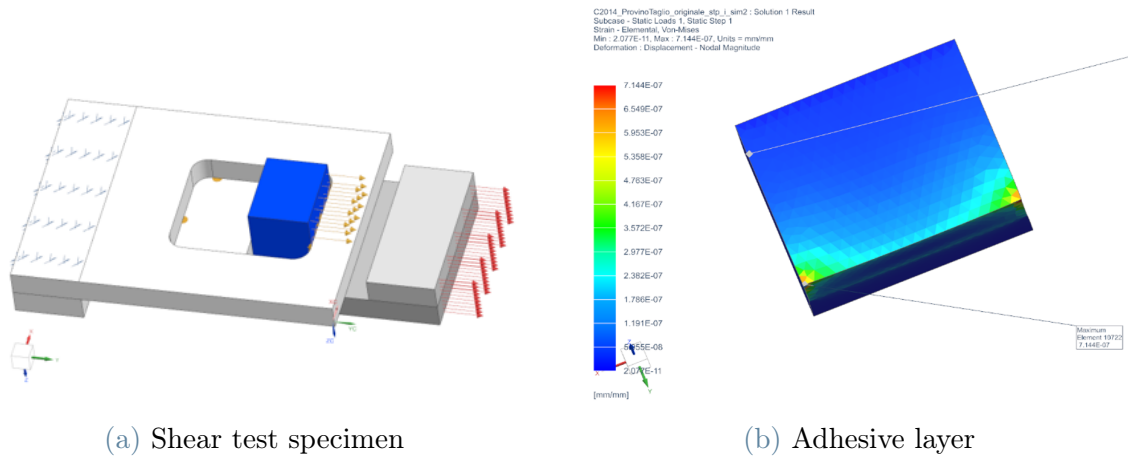


Figure 4.12: NOA88 simulation through penalty contact

#### 4.4.1. Thermoelastic analysis

Thermoelastic analysis is used to determine the state of the telescope's components following the change of temperature experienced in space by analyzing the lenses at the contact point with the adhesive. In this case, the analysis is required because of a manufacturing error: A little bit of UV-curable adhesive is inadvertently placed between the lens and the metal support to secure the lens while the structural adhesive cures, and will be removed after curing. However, with the particular geometry of this assembly the removal of the adhesive is particularly difficult. Typically, lenses are secured to the primary structure through the structural adhesives on a flexible support. This approach is employed to avoid the occurrence of contact between the lens and the metal structure. Consequently, our analysis focused on the additional stress at the new contact point where the lens is bonded directly to a large, rigid metal structure rather than a compliant area. This particular placement results in significantly higher thermal stresses, with computed values reaching approximately 60 MPa (Figure 4.13).

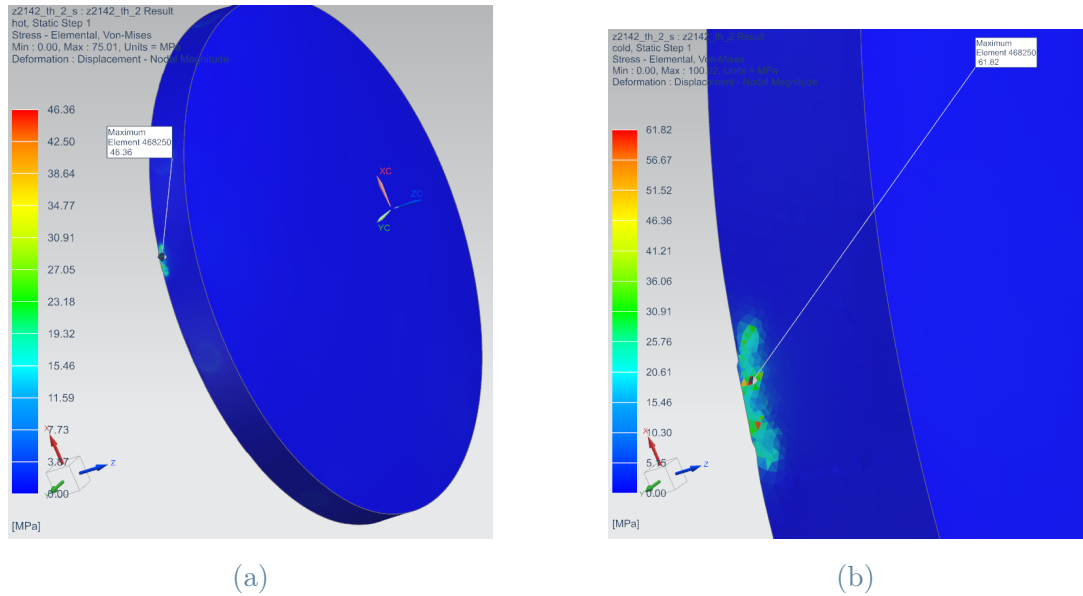


Figure 4.13: NOA 88 thermoelastic simulation

Although this stress level is below the failure limit for Fused Silica, it provides an insufficient safety margin to prevent potential cracking. Therefore, it is recommended that the residual UV adhesive be removed using mechanical disassembly to ensure the optical integrity of the lens in operative conditions.

## 5 | Conclusions and future developments

This thesis has examined some of the numerous challenges associated with employing structural adhesives in space applications. The research demonstrates that adhesive performance is sensitive to several factors: surface treatment of the substrates, thermal mismatches between adhesives and bonded materials, and the precision of the manufacturing process. Experimental tests on substrate combinations have underscored that increased surface roughness can significantly enhance bond strength in case of structural epoxy adhesives while the opposite is true for optical adhesives. However, the variability in test results introduced by microdefects in bonding or substrate surfaces signifies the continued necessity of rigorous testing and investigation before production, in addition to the requirements of the established protocol.

Thermal effects further complicate adhesive performance. The differential coefficients of thermal expansion between the adhesive and substrates can induce stresses during thermal cycling in the challenging space environment, a critical concern for high-precision assemblies such as telescope lenses. Even slight thermal mismatches may lead to deformation or bond failure, emphasizing the importance of comprehensive thermal analysis in the design phase.

Manufacturing precision is another critical factor in this regard. The findings of our studies indicate that deviations in adhesive thickness, shrinkage, and assembly inaccuracies can generate residual stresses that compromise joint integrity. The employment of advanced simulation techniques has proven effective in predicting adhesive behavior under varying conditions and suggesting a change in the geometry of the component or the manufacturing process if necessary.

Looking forward, the field of adhesives for space applications continues to be a dynamic area of research. Future developments should focus on refining cohesive element models to better capture the behavior of strong, brittle adhesives and on developing robust databases that integrate all relevant factors (such as surface treatment methods, material properties,

and environmental conditions) to improve design predictability by improving the material characterization. Additionally, standardizing test procedures and employing automated surface treatment processes will be critical for achieving consistent results and ensuring long-term reliability.

In conclusion, while the current state of the art for adhesives implementation fulfills many requirements for space applications, advancements in material characterization, simulation accuracy, and manufacturing processes are essential to meet the evolving demands of the aerospace industry. This work, supported by direct experimental experience and advanced simulation methodologies, lays the groundwork for further innovation in this challenging yet critical field.

## Bibliography

- [1] *Scotch-Weld Epoxy Adhesive 2216 B/A*. 3M, 2024. URL [www.3M.com/structuraladhesives](http://www.3M.com/structuraladhesives).
- [2] B. Badr, M. Mokhtari, K. Madani, and H. Benzaama. Using a cohesive zone modeling to predict the compressive and tensile behavior on the failure load of single lap bonded joint. *Frattura ed Integrità Strutturale*, 13:112–125, 08 2019. doi: 10.3221/IGF-ESIS.50.11.
- [3] R. Campilho and T. Fernandes. Comparative evaluation of single-lap joints bonded with different adhesives by cohesive zone modelling. *Procedia Engineering*, 114:102–109, 2015. ISSN 1877-7058. doi: <https://doi.org/10.1016/j.proeng.2015.08.047>. URL <https://www.sciencedirect.com/science/article/pii/S1877705815016860>. ICSI 2015 The 1st International Conference on Structural Integrity Funchal, Madeira, Portugal 1st to 4th September, 2015.
- [4] R. D. S. G. Campilho, K. Madani, and C. Prakash. Advanced characterization of adhesive joints and adhesives. *Materials*, 15(20), 2022. ISSN 1996-1944. doi: 10.3390/ma15207347. URL <https://www.mdpi.com/1996-1944/15/20/7347>.
- [5] J. Chen, N. Ding, Z. Li, and W. Wang. Organic polymer materials in the space environment. *Progress in Aerospace Sciences*, 83:37–56, 2016. ISSN 0376-0421. doi: <https://doi.org/10.1016/j.paerosci.2016.02.002>. URL <https://www.sciencedirect.com/science/article/pii/S0376042115300166>.
- [6] P. Côté and N. Desnoyers. Thermal stress failure criteria for a structural epoxy. In A. E. Hatheway, editor, *Optomechanics 2011: Innovations and Solutions*, volume 8125, page 81250K. International Society for Optics and Photonics, SPIE, 2011. doi: 10.1117/12.893832. URL <https://doi.org/10.1117/12.893832>.
- [7] K. K. De Groh, B. A. Banks, and i. b. NASA Glenn Research Center. *MISSE-flight facility polymers and composites experiment 1-4 (PCE 1-4)*. NASA/TM ; 20205008863. National Aeronautics and Space Administration, Glenn Research Center, Cleveland, Ohio, 2021 - 2022.

- [8] *ECCOBOND 56 C*. Emerson and Cuming National Starch and Chemical Company, 2024. URL <https://www.spacematdb.com/spacemat/manudatasheets/ECCOBOND56C.pdf>.
- [9] T. Ghidini. Materials for space exploration and settlement. *Nature Materials*, 17, 09 2018. doi: 10.1038/s41563-018-0184-4.
- [10] *Araldite AV 138M with Hardner HV 998*. Huntsman, 2004. URL [www.araldite.com](http://www.araldite.com).
- [11] H. Khoramishad, A. Akhavan-Safar, M. Ayatollahi, and L. da Silva. Predicting static strength in adhesively bonded single lap joints using a critical distance based method: Substrate thickness and overlap length effects. *Proceedings of the Institution of Mechanical Engineers, Part L: Journal of Materials: Design and Applications*, 231 (1-2):237–246, 2017. doi: 10.1177/1464420716666427. URL <https://doi.org/10.1177/1464420716666427>.
- [12] P. A. C. V. C. B. I. F. W. G. M. K. F. S. M. S. D. S. C. B. Konstantinos Tserpes, Alberto Barroso-Caro and V. Rajčić. A review on failure theories and simulation models for adhesive joints. *The Journal of Adhesion*, 98(12):1855–1915, 2022. doi: 10.1080/00218464.2021.1941903. URL <https://doi.org/10.1080/00218464.2021.1941903>.
- [13] *EP29LPSP*. Masterbond Polymer Systems, 2024. URL [www.masterbond.com](http://www.masterbond.com). [techinfo@masterbond.com](mailto:techinfo@masterbond.com).
- [14] *EP30-2*. Masterbond Polymer Systems, 2024. URL [www.masterbond.com](http://www.masterbond.com). [techinfo@masterbond.com](mailto:techinfo@masterbond.com).
- [15] *EP42HT-2LO*. Masterbond Polymer Systems, 2024. URL [www.masterbond.com](http://www.masterbond.com). [techinfo@masterbond.com](mailto:techinfo@masterbond.com).
- [16] *Supreme 11HT-LO*. Masterbond Polymer Systems, 2024. URL [www.masterbond.com](http://www.masterbond.com). [techinfo@masterbond.com](mailto:techinfo@masterbond.com).
- [17] *UV24TKLO*. Masterbond Polymer Systems, 2024. URL [www.masterbond.com](http://www.masterbond.com). [techinfo@masterbond.com](mailto:techinfo@masterbond.com).
- [18] *UV26*. Masterbond Polymer Systems, 2024. URL [www.masterbond.com](http://www.masterbond.com).
- [19] P. Maćkowiak, B. Ligaj, D. Płaczek, and M. Kotyk. Verification of selected failure criteria for adhesive bonded elements with different stiffness through the use of methacrylic adhesive. *Materials*, 13(18), 2020. ISSN 1996-1944. doi: 10.3390/ma13184011. URL <https://www.mdpi.com/1996-1944/13/18/4011>.

- [20] *Norland Optical Adhesive 88*. NORLAND PRODUCTS INCORPORATED, 2024. URL [www.norlandproducts.com](http://www.norlandproducts.com).
- [21] *CV-1142*. Nusil, 2014. URL [www.nusil.com](http://www.nusil.com).
- [22] R. Quispe Rodríguez, W. P. de Paiva, P. Sollero, M. R. Bertoni Rodrigues, and Éder Lima de Albuquerque. Failure criteria for adhesively bonded joints. *International Journal of Adhesion and Adhesives*, 37:26–36, 2012. ISSN 0143-7496. doi: <https://doi.org/10.1016/j.ijadhadh.2012.01.009>. URL <https://www.sciencedirect.com/science/article/pii/S0143749612000103>. Special Issue on Joint Design 3.
- [23] J. A. B. P. N. R. D. S. G. Campilho, M. D. Banea and L. F. M. da Silva. Modelling of single-lap joints using cohesive zone models: Effect of the cohesive parameters on the output of the simulations. *The Journal of Adhesion*, 88(4-6):513–533, 2012. doi: 10.1080/00218464.2012.660834. URL <https://doi.org/10.1080/00218464.2012.660834>.
- [24] L. Ramalho, R. Campilho, J. Belinha, and L. da Silva. Static strength prediction of adhesive joints: A review. *International Journal of Adhesion and Adhesives*, 96:102451, 2020. ISSN 0143-7496. doi: <https://doi.org/10.1016/j.ijadhadh.2019.102451>. URL <https://www.sciencedirect.com/science/article/pii/S0143749619302003>.
- [25] S. J. A. B. I. K. M. P. E. C. Scott E. Stapleton, Bertram Stier and B. A. Bednarczyk. A critical assessment of design tools for stress analysis of adhesively bonded double lap joints. *Mechanics of Advanced Materials and Structures*, 28(8):791–811, 2021. doi: 10.1080/15376494.2019.1600768. URL <https://doi.org/10.1080/15376494.2019.1600768>.
- [26] J. Wirries and M. Ruetters. Methods for shrinkage measurement considering stress development of curing structural adhesives. *Proceedings of the Institution of Mechanical Engineers, Part D: Journal of Automobile Engineering*, 237(13):2986–2998, 2023. doi: 10.1177/09544070221103676. URL <https://doi.org/10.1177/09544070221103676>.
- [27] R. D. A. X. Zhao and L. F. M. da Silva. Single lap joints with rounded adherend corners: Experimental results and strength prediction. *Journal of Adhesion Science and Technology*, 25(8):837–856, 2011. doi: 10.1163/016942410X520880. URL <https://www.tandfonline.com/doi/abs/10.1163/016942410X520880>.
- [28] C. Yang, J. Tomblin, and Z. Guan. Analytical modeling of astm lap shear adhesive specimens. page 78, 02 2003.

- [29] E. Zappino, N. Zobeiry, M. Petrolo, R. Vaziri, E. Carrera, and A. Poursartip. Analysis of process-induced deformations and residual stresses in curved composite parts considering transverse shear stress and thickness stretching. *Composite Structures*, 241:112057, 2020. ISSN 0263-8223. doi: <https://doi.org/10.1016/j.compstruct.2020.112057>. URL <https://www.sciencedirect.com/science/article/pii/S0263822319337043>.

# A | Appendix A

## A.1. Market research tables

Here are the tables containing the adhesives mentioned for the market research:

| Adhesive name                | EP42HT-2LTE               | EP29LPSP                   | EP30-2          | Supreme 11HT-LO      | EC 2216 B/A Gray |
|------------------------------|---------------------------|----------------------------|-----------------|----------------------|------------------|
| Type                         | two-part epoxy            | two-part epoxy             | two-part epoxy  | two-part epoxy       | two-part epoxy   |
| Supplier                     | Masterbond                | Masterbond                 | Masterbond      | Masterbond           | 3M               |
| Temperature [°C]             | -269,15 ~+ 149            | -269,15 ~ +135°C           | -269,15 ~+149°C | -80°C~+204°C         | -50°C ~80°C      |
| Curing t temperature [°C]    | 24°                       | 54,4-65,5° 79,4° 93,3° 23° | 23°             | 23° 93,3°            | 24° 70°          |
| Curing time                  | 4-7 d                     | 8-10h 5-7h 3-5h            | 24-48h          | 24-36h 1-2h          | 7d 2h            |
| Viscosity [cps]              | moderately flowable paste | 500-1,500                  | 10000           | high viscosity paste | 75000-150000     |
| Pot Life/work life [minutes] | 60-90                     | 240-300                    | 20-40           | 20-25                | 90               |
| Tensile strength [MPa]       | 41,3- 48,2                | >55,16                     | 68-75           | 48,26-55,1           | 21,3             |
| Lap shear strength [MPa]     | 4,8-6,2                   | >15,17                     | 20-22           | 22-23,4              | 21,3             |
| CTE [ppm/°C]                 | 9-12                      | 45-55                      | 40-45           | 45-50                | 45 (<100°)       |
| TML                          | <0.1%                     | <0.1%                      | <0.1%           | <0.1%                | 0,77%            |
| CVCM                         | <0.01%                    | <0.01%                     | <0.01%          | <0.01%               | 0.04%            |
| Already available            | Yes                       | No                         | No              | No                   | Yes              |

Table A.1: Adhesive on the market (1). The data is derived from the datasheets: [15], [13], [14], [16], [1]

| Adhesive name                | V138M-HV998    | CV-1142                               | Eccobond<br>"Solder" 56C        | Norland 88       | UV24TKLO                                  | UV26            |
|------------------------------|----------------|---------------------------------------|---------------------------------|------------------|---|-----------------|
| Type                         | two-part epoxy | One-part,<br>solvent free<br>silicone | silver filled<br>two-part epoxy | single component | acrylic                                   | acrylic         |
| Supplier                     | Hutsman        | Nusil                                 | Henkel                          | Norland          | Masterbond                                | Masterbond      |
| Temperature [°C]             | ? - 120°       | -115°C to +232°C                      | -60°C to +175°C                 | -60°C to +90°C   | -51°C to +204°C                           | -51°C to +260°C |
| Curing temperature [°C]      | 23°<br>40°     | 25°                                   | 23                              | UV               | UV  | UV              |
| Curing time                  | 24h<br>16h     | 4h                                    | 6h                              | minutes          | minutes                                   | minutes         |
| Viscosity [cps]              | Thixotropic    | 7000 ± 1000                           | high viscosity paste            | 250              | 30,000-45,000 (23°)<br>5,000-15,000 (40°) | 250-1,500       |
| Pot Life/work life [minutes] | 35             | 20                                    | 20                              | 5                | 5   | 5               |
| Tensile strength [MPa]       | –              | 2                                     | 15                              | 13,8             | >55                                       | 48-55           |
| Lap shear strength [MPa]     | 9,7            | 1,4                                   | 5,5                             | 7                | 20  | 20              |
| CTE [ppm/°C]                 | 67             | 320                                   | 36                              | 45-55            | 45-55                                     | 50-55           |
| TML                          | 0.84%          | 0.33%                                 | 0,23%                           | <0.1%            | <0.1%                                     | <0.1%           |
| CVCM                         | 0.02%          | 0.04%                                 | 0,01%                           | 0.01%            | <0.01%                                    | <0.01%          |
| Already available            | Yes            | Yes                                   | Yes                             | Yes              | No  | No              |

Table A.2: Adhesive on the market (2). The data is derived from the datasheets: [10],[21],[8],[20],[17],[18]

## A.2. Adhesive Datasheets

Datasheets of the adhesives used in this thesis can be found in the bibliography

## List of Figures

|      |  |    |
|------|--|----|
| 1.1  | Adhesive failure . . . . .   | 4  |
| 1.2  | Cohesive failure . . . . .   | 4  |
| 1.3  | Mixed failure . . . . .  | 4  |
| 1.4  | Stress distribution in adhesive length . . . . .                           | 6  |
| 2.1  | Zernike deformation map . . . . .  | 22 |
| 2.2  | Zernike coefficients variation . . . . .                                   | 22 |
| 2.3  | Zernike deformed surface . . . . .   | 22 |
| 3.1  | Tensile test specimen . . . . .  | 24 |
| 3.2  | Tensile test results. Mean value: 20 MPa; Standard Dev.: 0.97 MPa . . .    | 25 |
| 3.3  | Difference in tensile performance for different surface roughness. . . . . | 26 |
| 3.4  | Comparison in tensile strength for different cure process . . . . .        | 27 |
| 3.5  | Stress distribution model of adhesive layer . . . . .                      | 27 |
| 3.6  | Shear test simulation model . . . . .                                      | 28 |
| 3.7  | Shear test specimen . . . . .  | 29 |
| 3.8  | Shear test results . . . . .   | 29 |
| 3.9  | Shear test simulation . . . . .  | 30 |
| 3.10 | Shear test simulation of the two adhesive areas configurations . . . . .   | 31 |
| 3.11 | FE Models of adhesive spot . . . . .                                       | 32 |
| 3.12 | Convergence vs. n° of elements . . . . .                                   | 32 |
| 3.13 | Shear test specimen . . . . .  | 34 |
| 3.14 | Difference in shear performance for different surface roughness . . . . .  | 34 |
| 3.15 | Glue spots analysis on a constrained lens . . . . .                        | 35 |
| 3.16 | Tensile test specimen . . . . .  | 36 |
| 3.17 | Tensile test results . . . . .   | 37 |
| 3.18 | Shear specimen . . . . .   | 37 |
| 3.19 | Shear test results . . . . .   | 38 |
| 3.20 | Shrinkage simulation . . . . .   | 40 |
| 3.21 | Thermoelastic analysis with CTE defined with temperature . . . . .         | 41 |

|      |   |    |
|------|---|----|
| 3.22 | Thermoelastic analysis with fixed CTE . . . . .                                 | 41 |
| 3.23 | Stress in the optical fiber vs. Maximum stress allowable in the fiber . . . . . | 43 |
| 3.24 | Optical fiber bending at the tip . . . . .                                      | 44 |
| 4.1  | Shear test results . . . . .  | 48 |
| 4.2  | Adhesive layer model . . . . .  | 49 |
| 4.3  | Stress induced in the lens by the adhesive comparison in different scenarios    | 51 |
| 4.4  | Finite element model of the lens fixed to the barrel . . . . .                  | 51 |
| 4.5  | Elements in the structured mesh . . . . .                                       | 53 |
| 4.6  | Convergence . . . . .   | 53 |
| 4.7  | Tensile test results . . . . .  | 54 |
| 4.8  | Shear test results . . . . .  | 55 |
| 4.9  | Adhesive failure in RTV566 . . . . .  | 56 |
| 4.10 | Tensile test results . . . . .  | 57 |
| 4.11 | Shear test results comparison . . . . .   | 58 |
| 4.12 | NOA88 simulation through penalty contact . . . . .                              | 59 |
| 4.13 | NOA 88 thermoelastic simulation . . . . .                                       | 60 |

## List of Tables

|     |   |    |
|-----|---|----|
| 3.1 | Structural adhesives examined . . . . . | 23 |
| 4.1 | Silicone adhesive comparison . . . . .  | 50 |
| A.1 | Adhesive on the market (1) . . . . .    | 68 |
| A.2 | Adhesive on the market (2) . . . . .    | 69 |



## Acknowledgements

This thesis is the result of years of hard work at Politecnico di Milano, a university that has welcomed me and pushed me to my limits. I would like to thank all the professors and mentors who helped me achieve this, especially Fabrizio, my supervisor in the company, and Prof. Grande, my thesis supervisor, from whom I still have a lot to learn. I would like to express my deepest gratitude to my family for their unconditional support and encouragement in times of need. In particular, I would like to acknowledge my mother, father, brother and grandfather, who have been a source of inspiration in my pursuit of a career in engineering. I would like to express my deep gratitude to my friends, especially Adi, Omar, Nil and Federico. Finally, I should like to express my deepest thanks to Chiara, whose help and unfailing support in times of uncertainty have been crucial to my accomplishments.

